IOWA STATE UNIVERSITY
Digital Repository

2013

Finite Element Analysis of a Levee

Elizabeth Roesler Shelman
Iowa State University

Recommended Citation

Finite element analysis of a levee

by

Elizabeth Roesler Shelman

A thesis submitted to the graduate faculty

in partial fulfillment of the requirements for the degree of

MASTER OF SCIENCE

Major: Civil Engineering (Geotechnical Engineering)

Program of Study Committee:
Vernon Schaefer, Major Professor
Jeramy Ashlock
Fouad Fanous

Iowa State University

Ames, Iowa

2013

TABLE OF CONTENTS

LIST OF FIGURES

LIST OF TABLES

ACKNOWLEDGEMENTS

ABSTRACT

A finite element analysis was used to examine the lateral soil deformation behavior of soft soils during the construction of levee improvements along the Sacramento River East Levee (SREL) in the Natomas Basin just north of Sacramento, CA. After Hurricane Katrina in 2005, it was found that Sacramento had the greatest risk of flooding due the ageing and inadequately maintained levee systems. An executive order was declared and agencies began to evaluate and mitigate levee conditions. Sacramento Area Flood Control Agency (SAFCA) evaluated the levee conditions and then designed and executed levee improvements along a 10 mile stretch of the SREL from 2005-2011. To meet United States Army Corps of Engineers Standards, a new adjacent levee was required. For underseepage control for much of this length, a soil-bentonite cutoff wall (SB wall) under the future adjacent levee crest was to be excavated near the toe of the existing 2H:1V embankment. Prior to construction, inclinometers were installed at the adjacent levee toe and between the existing levee and slurry trench. Inclinometer data showed unexpected horizontal movements of up to 10 mm, away from the trench during the excavation under a bentonite-slurry mixture. After the soil-bentonite fill was placed, horizontal movements shifted towards the trench and greater than 25 mm of movement were observed to distances nearly two times the slurry trench depth from the cutoff wall alignment.

A study was developed to evaluate the key parameters affecting lateral deformation of the soft Sacramento River soils. The model was implemented in multiple steps to mimic the actual phased construction performed in the field. The steps included the initial working platform fill, excavation and subsequent filling of the trench with bentonite-slurry mixture, backfilling of the trench and final filling of the embankment. Soil and ground conditions in the model were

established from field and laboratory testing. Developing accurate stress-strain response was crucial to understanding the key parameters attributing to the lateral movement in the field. Results obtained in the model were compared with recorded field measurements determined from inclinometer readings. The initial movement away from the trench was likely dependent on stiffness of the natural deposits. The amount and rate of lateral movement toward the trench, after backfilling, trended with horizontal consolidation of the soil-bentonite backfill. This study can be useful in understanding the lateral behavior of the soft soils for making lateral deformation predictions in the case of construction excavations.

CHAPTER 1: INTRODUCTION

1.1 Historical Background

Henry Petroski, a Civil Engineering professor at Duke University, defines a levee as an "elongated naturally occurring ridge or artificially constructed fill or wall, which regulates water levels. It is usually earthen and often parallel to the course of a river in its floodplain or along low-lying coastlines" (Petroski, 2006). It has been estimated that the United States has 100,000 miles of levees (ASCE, 2013). Many of them were originally used for agricultural purposes, but as cities have grown they have come to serve as a means of flood control for larger communities.

Since Hurricane Katrina in 2005, the condition of the levees around the United States has been a topic of increased concern and speculation. Since that event, much effort has gone into the evaluation and improvement of our levees. Sacramento, California was identified as having an unacceptably high risk of flooding, greatest of any major city in the country due to its location at the confluence of two major rivers the Sacramento River and the American River, shown in Figure 1-1, and the city's outdated levee systems. Records of severe flooding, causing damage to the city's infrastructure, go back over 150 years since the formation of the city in the mid 1800's (SAFCA, 2008). Most residents in the city live at or below the river level. It has been hypothesized that in the worst case scenario, if the levees failed, parts of the city would be underwater in a matter of hours (Weisner et al., 2012). A major flood could cause many deaths and take a large toll on the local economy.

The levee system in the Sacramento area was constructed in the late 1800's to early 1900's. They were not built to current engineering standards, and little care was given to the suitability of the foundation soils. Although improvements and remediation to the levee systems around Sacramento have been ongoing since before Hurricane Katrina struck New Orleans,

Katrina brought about a new nationwide awareness of the issue and concern for our levees. In 2006 the governor of California declared a state of emergency for the California levees. He issued an executive order for agencies to ramp up evaluation and mitigation of the levees.

Figure 1-1: Map of Sacramento River [accessed from Demis Map Server (2013)]

As the evaluation of levees in Sacramento progressed, they were assessed to see if they met the United States Army Corps of Engineers (USACE) standards for the 100-year flood elevation or greater. Cues were also taken from what was learned from studying the New Orleans levees after Katrina. Following the assessment, construction to repair and mitigate the levees began.

To ensure that levees are able to meet the desired performance, instrumentation such as inclinometers, piezometers, and settlement sensors are used before, during and after the

construction process. This instrumentation, however, must be checked on a regular basis such that sufficient engineering judgment can be applied in a timely manner to irregularities in the data. An example of such irregularities could include excessive settlement, lateral deformations, or abrupt changes in the groundwater table; changes in the ground that may affect the effectiveness of the design. One such irregularity was found on the Sacramento River East Levee (SREL) during the construction of a soil-bentonite cutoff wall.

1.2 Sacramento River East Levee

One of the levee systems near Sacramento that was identified as an area of concern was the SREL. The SREL is part of a system of levees in the Natomas Basin, shown in yellow in Figure 1-2. The Natomas Basin is 220 km^2 and includes not only prime agricultural land and commercial developments but also major infrastructure, including the Sacramento International Airport, Power Balance Arena, Interstates 5 and 80, and numerous recent residential subdivisions with over 10,000 homes.
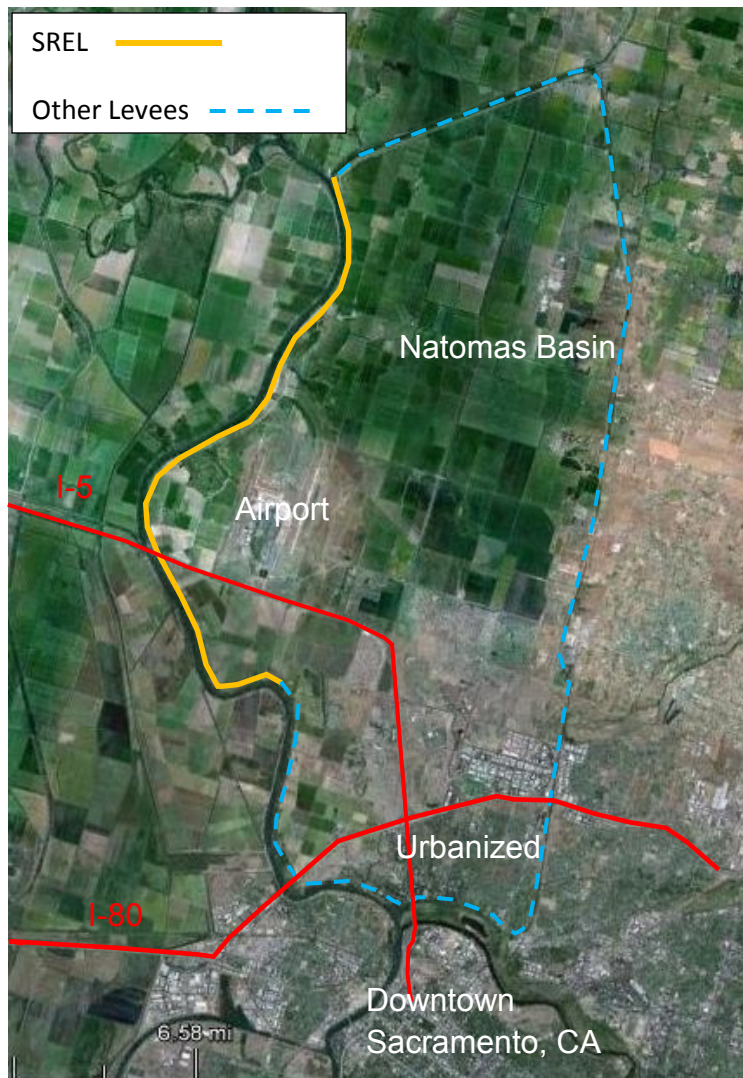
Figure 1-2: Map of Natomas Basin showing levee locations

1.2.1 Background

The SREL was constructed in the early 1900's with a dragline used to excavate a trench about 6 to 12 feet deep along the centerline of the levee alignment. Hydraulic dredging operations placed material from the adjacent Sacramento River bottom into the excavation area between the levees. This material consisted predominately of sands. The final levee

configuration was achieved by covering the dredged sand with the adjacent levee materials. These materials consisted predominately of silt, clay, and fine sand.

1.2.2 Geology

Mapping by Helley and Harwood (1985) indicates the entire levee is underlain by alluvium and basin deposits. Several well-defined paleo-channels were identified intersecting and adjacent to SREL. These deposits were formed by the pre-levee Sacramento River and represent historical and Holocene river channels that were deposited, incised/eroded, and overlain by younger deposits as the rivers meandered across their flood plains. These remnant river features and alluvial deposits may be filled to partially filled with loose granular or soft fine-grained sediments.

1.2.3 Construction and Mitigation

Several remedial and emergency flood repairs have been required over the years and more recently it was assessed that SREL does not meet USACE criteria to meet 100-year and larger flood elevation conditions (Kleinfelder, 2010).

From 2005 to 2011, construction occurred to bring SREL up to the USACE current levee standards per USACE EM 1110-2-1913 (USACE, 2000). As a part of this new construction, an adjacent levee was constructed to meet geometry standards next to the existing levee. In some areas soil-bentonite cutoff walls were installed to prevent underseepage, and seepage berms were constructed on the landside of the levee.

In SREL the purpose of the slurry wall was to mitigate underseepage conditions which could lead to levee instability by piping and boiling conditions. By cutting off permeable layers in the levee, forcing the water to flow under the wall, water pressures are unable to build up

underneath the levee during flood conditions. A typical SREL cross section with a soil-bentonite slurry wall is shown in Figure 1-3 below.

The SREL slurry walls were constructed below the new, adjacent levee, near the location of the existing levee toe. The two methods used to construct the walls included trenching, for walls less than 100 feet in depth, and the deep–mix-method (DMM), for walls greater than 100 feet in depth. Cutoff walls varied in depth based on the local subsurface conditions and ranged between 20 to 125 feet.

During construction, instrumentation was installed in the levee to monitor subsurface conditions during the construction and for long term. Instrumentation included inclinometers, piezometers, and settlement sensors, which monitored lateral movement, porewater pressures, and vertical movement respectively. The typical location of the inclinometers are shown in Figure 1-3.
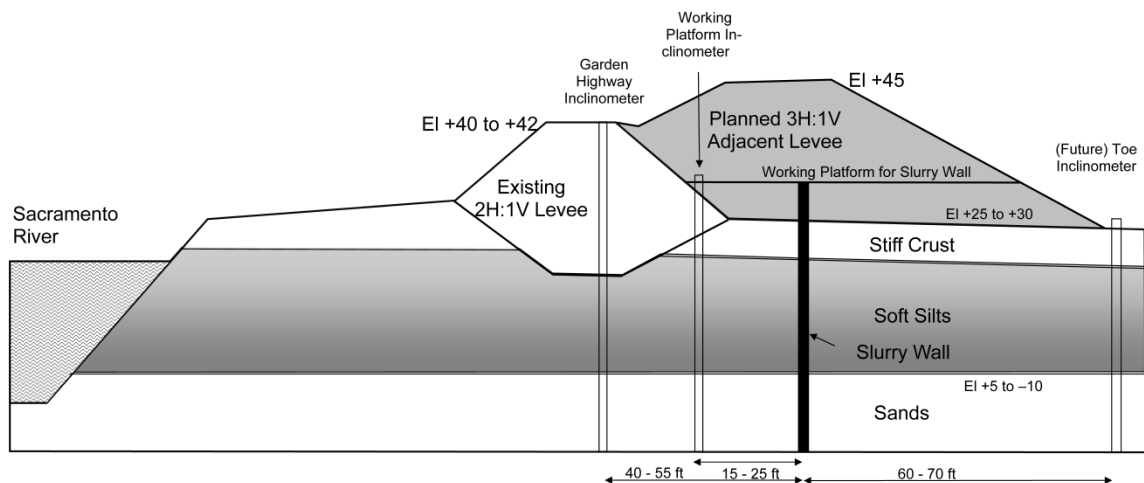
Figure 1-3: Typical SREL cross section with SB wall and location of inclinometers

1.3 Objectives and Scope of Research

During construction of the soil-bentonite slurry wall the inclinometer profiles adjacent to the cutoff wall showed lateral behavior which coincided with the construction steps of the wall. When the trench was excavated and a bentonite-slurry mixture was placed in the trench for stability, inclinometers recorded the movement of the soft soils away from the trench. The movement away from the trench was counter to what was expected. This movement continued to progress until the trench was completely backfilled with the soil-bentonite slurry mixture; unexpected horizontal movements of up to 10 mm were recorded. At this point in time, the movement recorded by the inclinometers showed that the adjacent soils started moving toward the excavation. Greater than 25 mm of movement were observed to distances nearly two times the slurry trench depth from the cutoff wall alignment. The deformation that occurred corresponded to the location of soft soil layers. Figure 1-4 below shows typical inclinometer profiles for a SB slurry wall and a DMM wall.
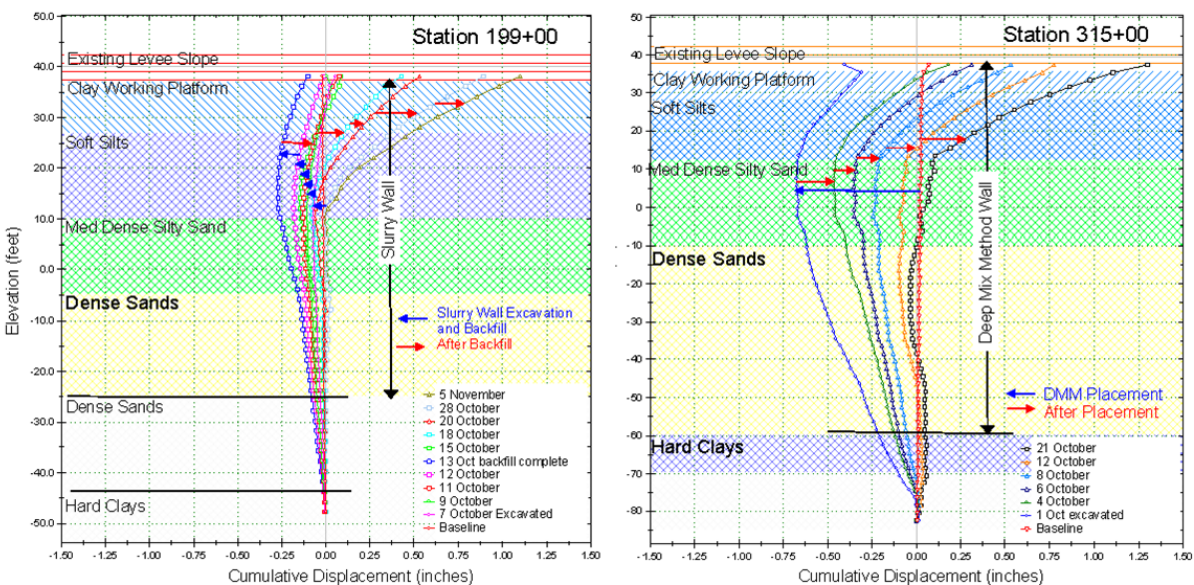
Figure 1-4: Typical Inclinometer Cumulative Deflection Profiles for a) Slurry Wall and b) DMM Wall

Due to the unanticipated amount and direction of the lateral soil movement, a finite element analysis was developed in order to understand the material behavior properties due to the interaction of the soil-SB slurry and soil-SB fill. The development of the model was done through a series of steps including: the development of a cross section; development of soil constitutive models and soil parameters; entering the data into the modeling software; modeling cutoff wall installation and levee construction; analyzing the results; and comparing the results with the data from the field.

1.4 Overview of Thesis

The remainder of the thesis discusses in detail the aforementioned project. The discussion begins with an overview of this project in the introduction by providing background information and the scope of research undertaken by this study. The second chapter provides detailed literature review regarding past research of the same nature that has been performed. Chapter three gives a thorough description of the modeling process. The results of the modeling and a discussion of the results are presented in detail in Chapter four. The fifth chapter presents the conclusions determined upon completion of this project

CHAPTER 2: LITERATURE REVIEW

2.1 Introduction

Using information collected for this literature review, the design and construction of a soil-bentonite cutoff wall is discussed in this chapter. Next, case-histories of deformation due to the construction of a soil-bentonite slurry wall are presented, as well as a review of finite element models of the deformation due to the construction of a soil-bentonite slurry wall that have previously been performed by others. Last, an overview of finite element modeling is given, including changes that have occurred in the past twenty years that have increased the capabilities of finite element modeling programs.

2.2 Soil –Bentonite Slurry Cutoff Wall Design

An engineering application of a soil-bentonite (SB) slurry wall is to provide an impermeable barrier. The first records of this type of slurry wall being constructed were from the USACE in early 1970's in California (Xanthakos, 1994). This type of wall is typically composed of a bentonite, soil, and water mixture.

The design depth and alignment of the trench is based on the purpose of the wall, as well as the site geology and groundwater conditions. Specifications for construction are written and focus on quality control efforts including: contractor qualifications, bentonite material properties, water quality, bentonite slurry properties, backfill properties, trench excavation methods, and soil backfill mixing and placing procedures. A stability analysis is typically performed to determine the factor of safety of failure of the trench supported by the slurry and help guide the aforementioned specifications.

Design procedures focus on the permeability of the soil-bentonite and the stability of the trench. The design is highly based on experience. Much of the research performed on soil-bentonite slurry walls is performed in these areas. Little focus has been given to the stress-state of the material during and after the construction of the wall.

2.3 Slurry Cutoff Wall Construction Procedures

The construction procedure for a SB slurry wall are as follows: A trench is excavated typically with a backhoe fitted with the appropriate size stick-and-boom for the design depth of the wall and appropriate size bucket for the design width, generally two to five feet (D'Appolonia, 1980). If deeper penetration of the earth is required than is capable with a backhoe, the construction is either performed by supplementing the backhoe excavation with clamshell excavation, or another type of construction method like deep soil mixing is employed. The soil excavated from the trench is replaced with bentonite slurry, which is mixed prior to use at an onsite location. The purpose of the slurry is to maintain trench stability through the construction. The slurry is typically composed of water mixed with 4-6% bentonite by weight (Barrier, 1995). The unit weight of the slurry is required to be larger than unit weight of water and in its pure form typically ranges from 64 to 70 pcf (Barrier, 1995). Requirements for the height of the slurry in the trench are that it to be at least a few feet above the water table and a few feet below the top of the trench. Keeping the soil above the water table allows for slurry to permeate into the adjacent soil, forming a "filter cake" (Filz et al. 1997). A filter cake is a thin layer of impermeable bentonite that forms along the sides of the trench; it contributes to the stabilization of the trench when the lateral pressure of the slurry acts against it.

The backfill mixing and filling typically occurs near the side of the trench. While the slurry trench is being excavated at one end, soil-bentonite backfill is placed at the other end with

a clamshell or pushed in the trench creating a gradual slope. The backfill displaces the slurry due

to its higher density. The material is composed of the slurry, removed from the trench, mixed

with the spoils from the trench. Sometimes offsite material is brought in order to meet backfill

specifications or to replace excavated soils that may be contaminated. The hydraulic conductivity

of the backfill typically ranges from $1x10^{-7}$ cm/s to $1x10^{-8}$ cm/s (Barrier, 1995), but has been

recorded to be even smaller in some cases.
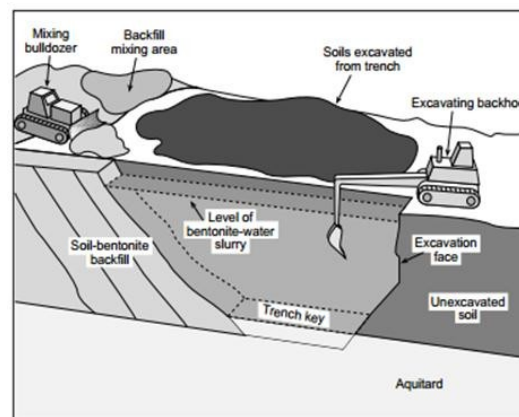
Figure 2-1: Soil Bentonite Cutoff Wall Operation [from Rumer and Ryan, 1995 as presented by Evans, 1995]

2.4 Case Histories of Deformation due to the Construction of a Soil-Bentonite Slurry Wall

In the literature, case histories were found that document deformations due to the

construction of soil-bentonite slurry walls. Manasquan dam in New Jersey was constructed with

a soil-bentonite slurry wall. Khoury et al. (1992) presents the vertical deformation data recorded

from the site; the deformation recorded was due to the consolidation of the soil-bentonite

backfill. The wall was constructed in two parts, a lower and an upper. The lower portion of the

wall was an average of 56 feet in depth and the upper portion of the wall was an average of 18

feet in depth. The upper wall was keyed three feet into the lower wall. The wall was three feet or

five feet in thickness depending on the location. Vertical settlement was measured by surveying settlement plates and borros points. The presented data showed a maximum settlement of 6.6 feet in the five-foot thick wall, with strains ranging from three to four percent. The maximum settlement in the three-foot wall was 3.2 feet, with strains ranging from seven to nine percent.

Vertical and lateral deformation recorded in the field during all stages of the SB wall construction at a site in Mountain View, California was documented by Baxter (2000). The SB wall was being constructed as a means of isolating a contaminated area and preventing contamination of local groundwater. Inclinometers and settlement sensors were installed at the site. Over the course of the construction and a consolidation period, up to 0.3 feet of vertical movement and 0.2 feet of horizontal movement was recorded. The majority of the deformation was due to the consolidation of the soil-bentonite backfill. This research is further discussed below as it pertains to finite element modeling below.

2.5 Summary of Finite Element Modeling in Soil-Bentonite Slurry Walls

Research on deformation modeling of a soil-bentonite slurry wall is very limited. Three studies were found in the literature that took place between 1994 and 2000.

The earliest study documented was performed by Clark (1994). The aim of the research was to study stress-transfer during soil-bentonite consolidation and the possibility of fracturing of the soil-bentonite cutoff wall. The cross section consisted of a soil-bentonite cutoff wall constructed into existing ground and then a levee was built on top of it. The constitutive model used was the Mohr-Coulomb elastic-plastic model. The following steps were used to model the construction. First, initial stresses were established using gravity forces and a coefficient of lateral earth pressure (K_o) of 0.5. Second the properties of bentonite slurry replaced the

properties of the alluvial soils in the area of the trench in order to represent the excavation of the trench under bentonite-slurry. The filter-cake on the sides of the trench was modeled as a frictional interface between the trench and the wall. Last, the properties of the bentonite slurry were changed to properties of the soil-bentonite fill incrementally in order to represent the backfilling of the trench. The computed results indicated that little lateral deformation occurred during the construction of the trench and that soil-arching occurred in the upper 5 meters of the soil-bentonite, but that these arching conditions were broken once consolidation occured.

Another finite element study was briefly mentioned in Barrier (1995). This study was used to model the consolidation stresses in a soil-bentonite slurry wall. Few details of the process and cross section are discussed, but the author notes that the problem was "imperfectly modeled." The program used could not simulate the excavation process with the bentonite slurry or the displacement of the slurry with soil-bentonite backfill. Also, parameters for the embankment soils were chosen based on typical values, as testing on the soil was not available. The author also mentions that there was not a method utilized between soil-bentonite elements at the trench wall and elements of the native ground to allow sliding to occur. Nevertheless, vertical effective stresses in the center of the soil-bentonite slurry wall correlate well with results obtained from dilatometer testing performed in the wall.

An aforementioned study by Baxter (2000) documents the development of a finite element model created in attempt to capture all the behavior of vertical and lateral deformation recorded in the field during all stages of the SB wall construction The modeling of the SB wall was of interest due to vertical and lateral movements that occurred during and after the construction that caused a nearby semiconductor manufacturing operation to become unusable.

A wealth of data was available for the study. Data included two inclinometers installed at the site for monitoring purposes, detailed construction documentation and SB material testing, as well as a geotechnical study and testing performed on the local soils.

The finite element program SAGE (Bentler et al. 1998), developed at Virginia Tech University, was used for the finite element analysis. SAGE, an acronym for the "static analysis of geotechnical engineering problems," uses a 2-D finite element method for plane strain and axisymmetric conditions. Newton-Raphson iteration is used in the SAGE program to solve non-linear finite element equations, which is appropriate for non-linear soil models. A coupled porewater pressure and deformation analysis was chosen in SAGE for the trench construction steps. An uncoupled analysis was used to establish initial stresses prior to the trench construction.

Initial conditions were modeled to establish preconstruction stresses. All phases of the construction were then modeled, which included the excavation of the trench with SB slurry material, backfilling of the trench with SB fill, and consolidation of the SB fill of the construction of the wall. Each aforementioned step was broken into substeps in SAGE. A total of 33 steps were modeled. First, in step one, the initial stresses were assigned in the model. For the second step a surcharge was applied and then removed in the third step. Step four involved reassigning horizontal effective stresses. Head boundary conditions were applied in step five and were varied in the following steps depending on the recorded water elevations from the field. In step six the excavation under the slurry bentonite mixture was modeled, followed by step seven where consolidation was allowed to occur. Steps eight through twenty-seven involve modeling of the backfilling of the trench. Last, in steps twenty-three through thirty-three the consolidation was modeled.

Constitutive models were used to model the behavior of the local soils. Laboratory testing performed on the soils and SB backfill material was used to develop the models. The constitutive model was chosen based on the material type. Sand was modeled using the Duncan and Chang (1970) hyperbolic model and clays were modeled using the Modified Cam Clay model. A constitutive model was created specifically for the SB material in this project; this model was termed the RS model and was based on the Modified Cam Clay model.

Successful calibration of the model was achieved to match the deformation recorded at the site. The calibrated model was then used to perform a parametric study of the site, varying site conditions in order to examine how this impacted the deformation.

2.6 Finite Element Method Modeling Software

The purpose of finite element analysis software is to solve partial differential equations that would otherwise be impossible to solve by hand in order to understand physical processes. Many physical processes such as stress analysis, fluid flow, heat transfer and electromagnetics can be modeled using the finite element method. Generally, the problem is broken into elements, connected by nodes (called a mesh) in order to obtain an approximate solution.

Typically in geotechnical problems finite element analysis is used to understand the physical processes of stress transfer and/or fluid flow in soil and rock or soil-structure interaction problems.

A huge drawback to finite element models for soil-bentonite slurry walls discussed in the previous section is the fact that the programs were more complicated to set up due to the computer programs, processors, and memory available to the users in the 90's and early 2000's, at the time of their research.

For example, in the SAGE program input files had to be generated by hand with a spreadsheet and a mesh generation program. Since then, more user-friendly, geotechnical specific programs have been developed. One of those programs is SIGMA/W 2007 (Geostudio, 2007). The program features preprogrammed soil constitutive models in which the user must determine the necessary parameters prior to running the model. While it was documented in Baxter (2000) that the SAGE program took six hours to run a model, SIGMA/W is able to process more complicated models in a matter of minutes. Performing a finite element model is more accessible to the working engineer today, provided he/she has the proper background and knowledge.

The program uses the following two dimensional equation (Equation 1) in conjunction with plane strain elements and Gauss-Legendre integration.

$$\int_v [B]^T [C][B] dv \{a\} = b\int_v <N>^T dv + p\int_A <N>^T dA + \{F_n\} \tag{1}$$

Where:
[B] = strain-displacement matrix,
[C] = constitutive matrix,
{a} = column vector of nodal incremental x- and y-displacements,
<N> = row vector of interpolating functions,
A = area along he boundary of an element,
v = volume of an element,
b = unit body force intensity,
p = incremental surface pressure, and
{Fn} = concentrated nodal incremental loads.

The program has five preprogrammed constitutive models and the option to create a user add-in constitutive model including: linear elastic, anisotropic linear-elastic, hyperbolic, Elastic-plastic, and Modified Cam-clay The models available to use depend on if the user chooses a total stress, effective stress with no pressure change or effective stress with porewater pressure change

conditions. The user is responsible for choosing the appropriate model for the material and developing the parameters specific to the model.

Several analysis types are available to use. The user can specify the analysis type based on the problem. Initial in-situ stress will need to be developed in the model; this is one of the analysis types. After the in-situ stresses are established the user can choose a load/deformation, coupled stress-pore pressure, volume change, stress redistribution, or dynamic deformation analysis type.

Another feature of the program is its ability to accommodate structural elements, allowing for soil-structure interaction analysis.

The program allows the user to model in stages where changes can be made in the model in separate steps. This functionality is appropriate to replicate steps in a construction process or changes that reflect field or test conditions.

In the next section the finite element analysis that was performed of the construction of the SREL slurry wall construction is discussed. It was performed in order to analyze the lateral deformation at different steps in the construction process. This analysis was developed using SIGMA/W. The constitutive models, analysis types, and the overall set-up of the finite element model are discussed in detail.

CHAPTER 3: DEVELOPMENT OF A FINITE ELEMENT MODEL FOR SREL WITH A SOIL BENTONITE WALL

3.1 Introduction

Chapter 2 discussed previous finite element analyses that involved deformation related to the construction of a soil-bentonite cutoff wall. This chapter presents the development of a finite element model deformation model for the construction of a SB cutoff wall in the SREL levee. As mentioned in Chapter 1, this model is of particular interest due to the unexpected movements of the soft soils adjacent to the wall. The development of this model includes: cross-section rationale and location details, development of the soil layering and soil parameters, and model set-up.

3.2 Cross Section Location

A cross section at Station 230+00 along SREL was chosen as the representative location for the analysis. This choice was based on the identification of soft soils, SPT blowcounts less than five in nearby boring logs, and visual classification in construction field reports. Another reason was the quantity and quality of instrumentation data at and near Station 230+00. More detail regarding the site is discussed in the following sections.

3.2.1   *Cutoff Wall Construction*

The soil bentonite slurry wall at 230+00 was built three-feet in width and to a depth of 60 feet (Elevation -25 feet) below the working platform (Elevation 35 feet). The soil-bentonite slurry wall was constructed using a Komatsu PC1250LC excavator with a long boom and stick and a three-foot wide bucket. As the material was excavated, bentonite slurry was simultaneously pumped from a mixing pond directly into the trench to fill in the area. Excavated soils from the trench, pea gravel, and slurry from the trench were mixed outside the trench to

create the soil bentonite fill material. The fill material was placed in the trench and displaced the slurry due to the relatively higher density. A two-foot thick soil cap was placed over the top of the wall after fill was completed. The wall was left to consolidate for at least 21 days before further adjacent levee fill was added.

3.2.2 Instrumentation

An inclinometer (SREL5A-230-R1) was installed on the working platform, approximately seven feet from the wall on the waterside. An inclinometer was installed at Station 231+00 (SREL5A-231-R1) at the adjacent levee toe about 100 feet away, landside of the wall. Adjacent to Station 231+00, a vibrating wire piezometer (SREL5A-231-C2) was placed in the soft soil material, approximately 10 feet from the wall, on the landside. SREL5A-230-R1 and SREL5A-231-T1 were installed to an elevation of approximately 38 and 35 feet, 10 and 13 feet below the depth of the slurry wall, respectively. All three instruments were installed after the completion of the working platform, but before the start of the wall excavation.

A settlement point was placed above the wall at Station 230+00 after the wall was backfilled. This point was surveyed every two to three days to monitor vertical consolidation settlement of the wall.
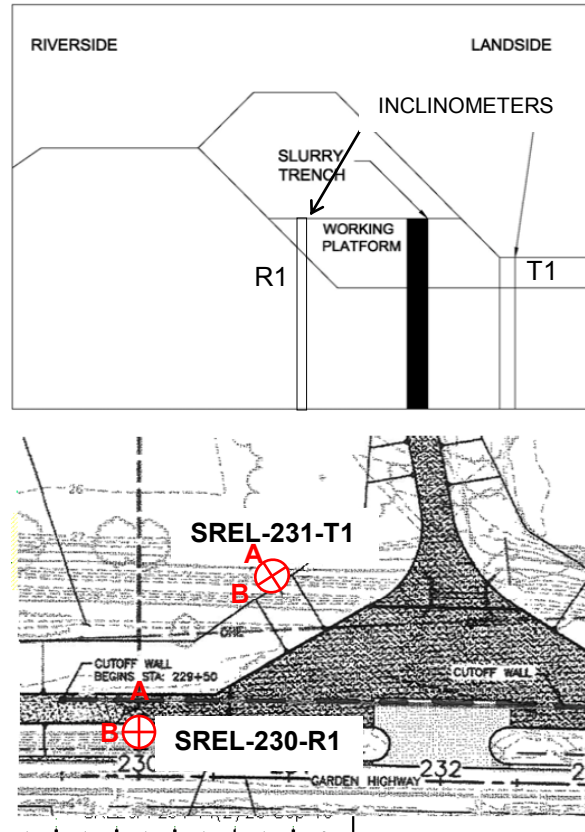
Figure 3-1: (a) Cross section showing inclinometers near Station 230+00. (b) Plan view showing inclinometers near Station 230+00

3.2.3   *Deformations of Ground Adjacent to the Cutoff Wall*

Readings from SREL5A-230-R1 show approximately 0.6 inches lateral movement of the soft soils outward relative to the excavation during the period of time from when the wall was excavated and filled with bentonite slurry on September 22, 2010 to the completion of the wall with soil-bentonite backfill on September 27, 2010. After the completion of the backfill, both SREL5A-230-R1 and SREL5A-231-T1 showed about 0.8 and 1.0 inches of lateral movement inward, transverse to the SB wall. Figures 3-2 and 3-3 below show the graphical results of each inclinometer. It is important to note that a reading at SREL5A-230-R1 (Figure 3-3) was not

performed during the 5 day filling period, so any outward movement that may have occurred during this time period was not accounted for at this location. It is also important to note the axis A, as shown in Figure 3-1, is not located perpendicular to the SB slurry wall. The deformation along axis A and axis B were resolved in order to obtain the cumulative deformation transverse to the SB slurry wall shown in Figure 3-3 below.
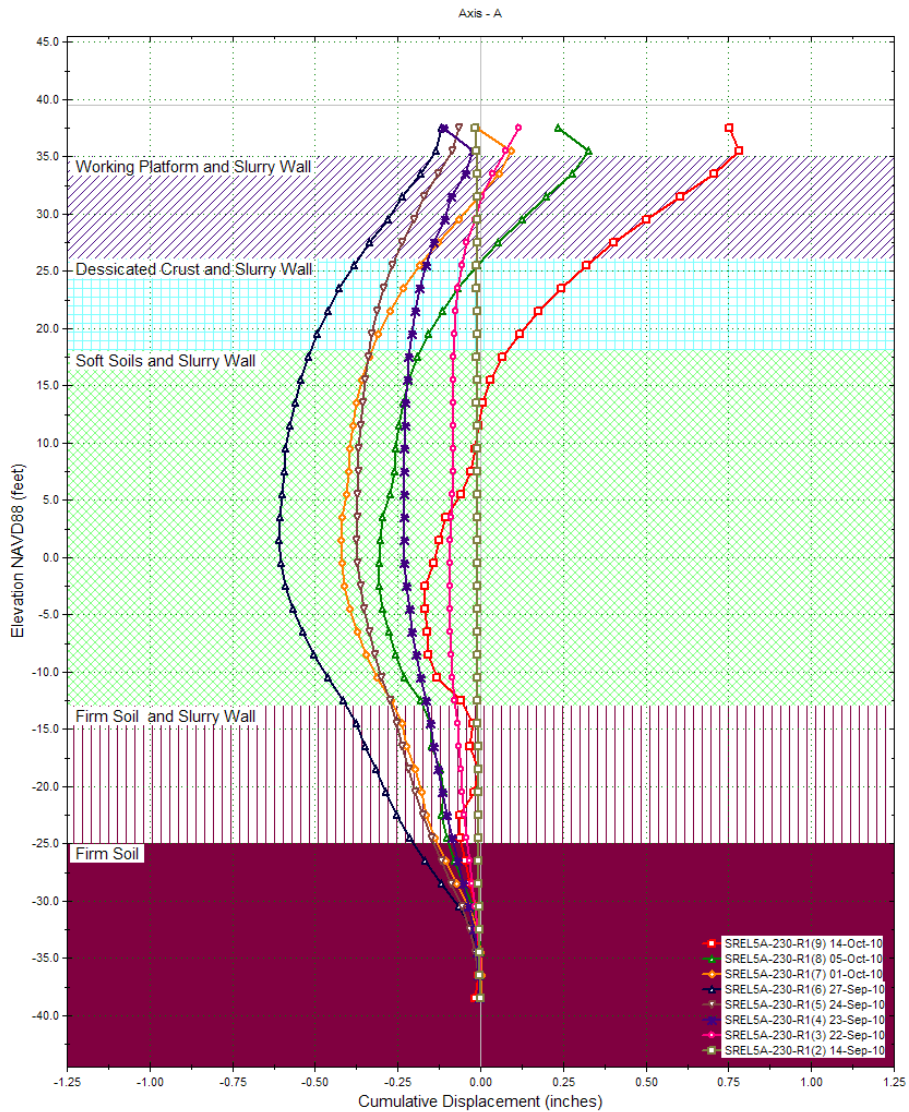
Figure 3-2: SREL5A-230-R1 Inclinometer Readings on Working Platform.
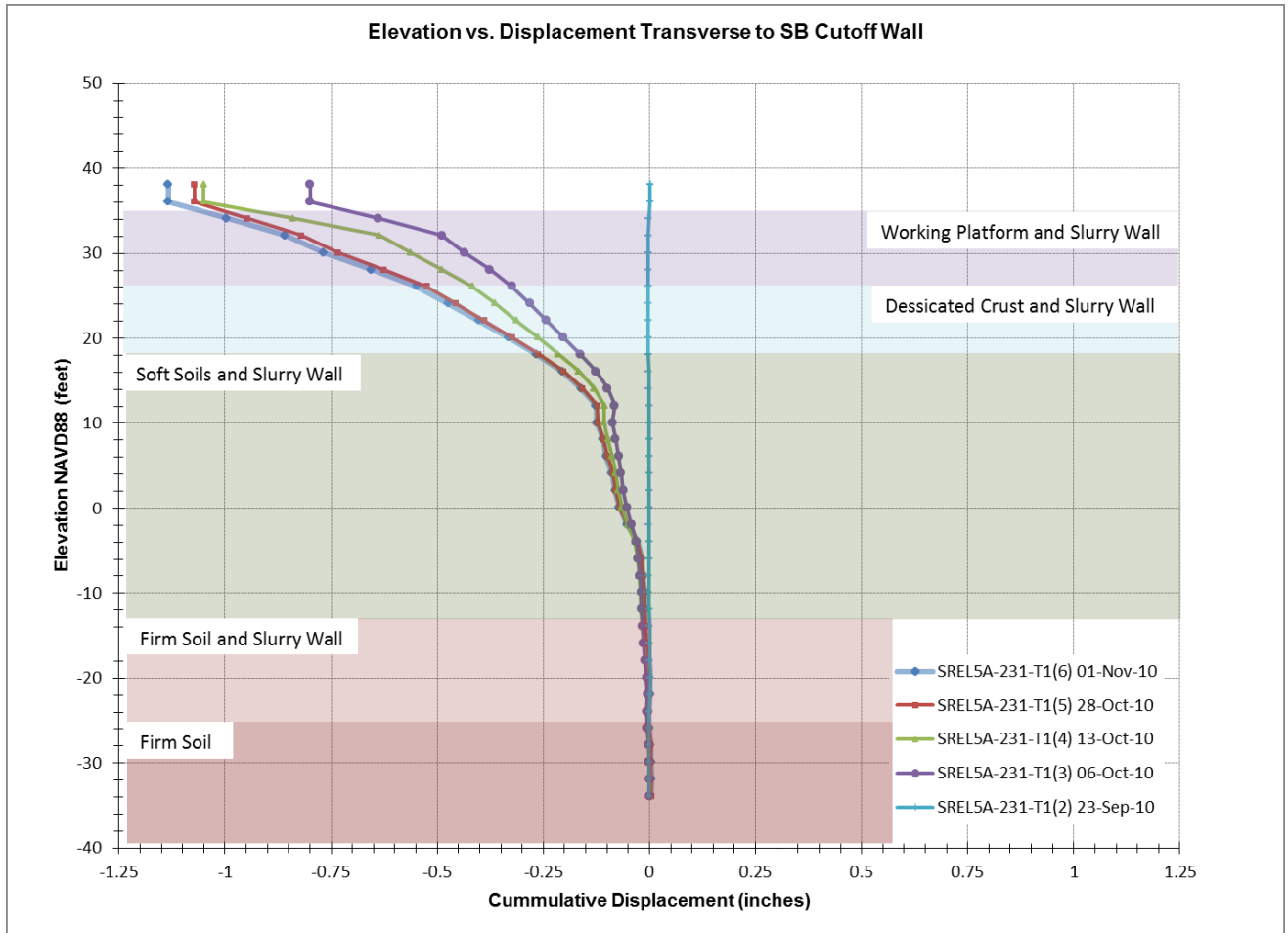
Figure 3-3: SREL5A-231-T1 Inclinometer Reading at Existing Levee Toe

3.3 Modeling Soil Conditions

Levee and the native alluvial soil layering used in the model was simplified and based on visual observations from the nearby boring logs, construction records, and testing data. Similar to the model shown in Figure 3-4, the model stratigraphy below the existing levee and constructed adjacent levee starts with a eight foot desiccated "crust" layer underlain by a 30 foot-previously aforementioned soft soil layer, which was divided into two materials, an upper, lower blow count, soft soil and a lower, relatively higher blow count material, soft soil. The upper and lower soft material is similar, but the lower layer is relatively stiffer and sandier. The soft soil layers

are underlain by a stiff soil, consisting mostly of sandy clay. It can be seen from the data that the majority of the lateral movement occurs in the soft soil and dissipates near the bottom of the inclinometers in the stiffer soil.
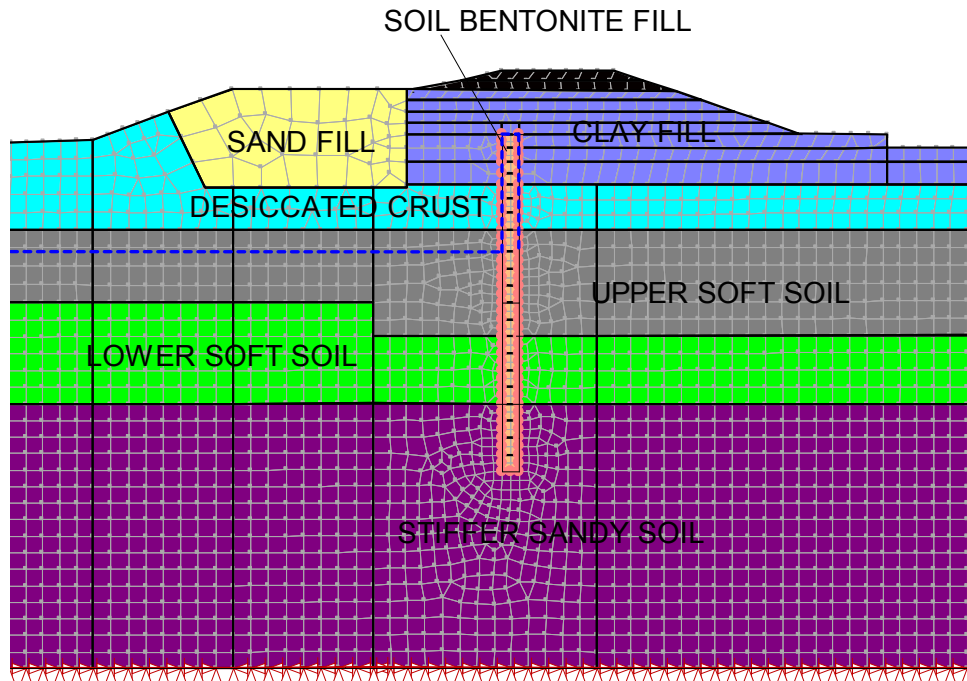
Figure 3-4: Cross Section of Model in SIGMA/W

Based on piezometer data from SREL2B-230-R1, buildup of porewater pressure in the soft silts dissipated quickly; therefore, it was decided that the model was to be run using effective stress conditions. The water table was set at 14 feet (NAVD88), which was a conservative estimate based on recorded data the time of the construction activities. Figure 3-5 below shows the local vibrating wire piezometers to the cross section. The Verona Gage, which is the elevation of the Sacramento River, is also shown along with the fill thickness at the site.
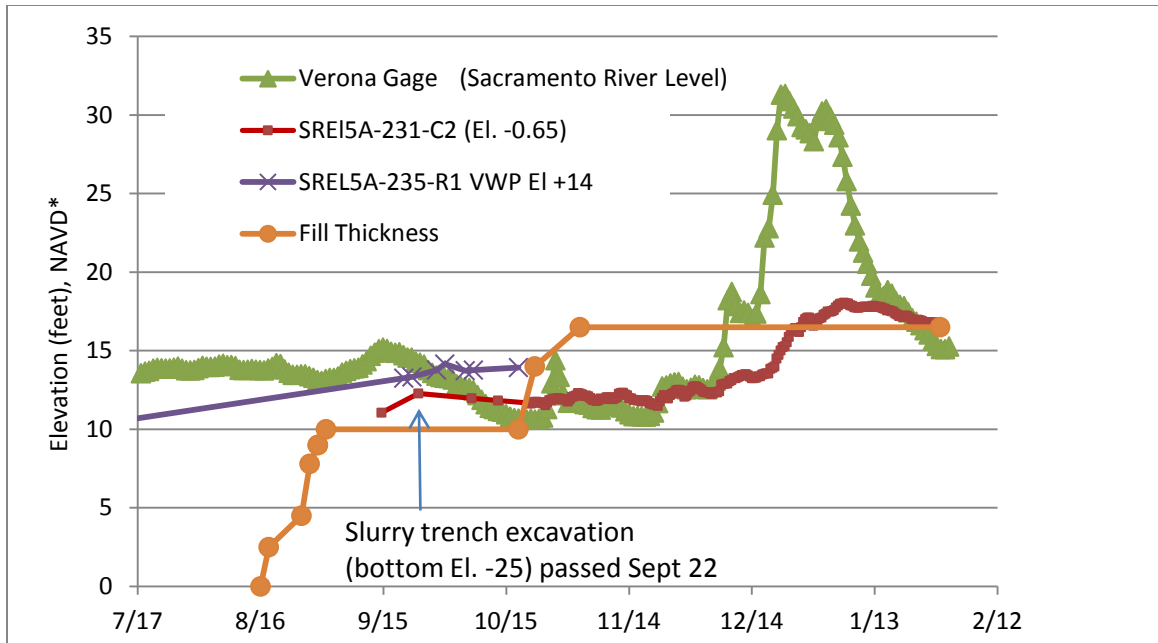
Figure 3-5: Summary of Water Table, VWP Piezometer, and Fill Elevation Data near Station 230+00

The model was limited to negative porewater pressures of 600 psf based on a report by Kleinfelder (2010b) which performed a detailed stability analysis and strength evaluation of the soft SREL soils .

3.4 Parameter Selection

The Duncan and Chang (1970) hyperbolic model was used for modeling each soil type. Parameters were developed according to Duncan et al. (1980) for each of the soil layers based on stress-strain curves from consolidated undrained shear tests on representative samples from nearby borings. The hyperbolic modulus method was used to estimate the Effective Modulus for the linear elastic method in SIGMA/W. K_o values were estimated from the Mayne and Kulhawy (1982) equation. OCR values and strength values used in the above equation were taken from prior reports and testing (Kleinfelder 2010, 2010a, and 2010b). All final parameters used in the model are shown in the attached Table 3.1. Initial parameter development is discussed below.

Existing Levee Core Material – Hyperbolic parameters were selected based on comparison values from Duncan et al. 1980, Table 5, for Sacramento River Sand.

Levee Fill Material – Strength testing data from the North Airport Borrow Site 2A (NAB2A) was collected for this research. The strength tests performed on samples from test pits labeled TP-AP-186 and TP-AP-17 were sampled in the upper one to two feet of the test pit. The reason for using these tests is NAB2A is where the adjacent levee fill was obtained from for the construction of SREL 2B, near Station 230+00 (the site of interest). Hyperbolic parameters were determined from the test performed on TP-AP-186 and showed a good fit to the actual data. An Rf of 0.89, K-modulus of 1000, and an exponent of 0.45 was determined from the hyperbolic curve fitting procedure.

Desiccated Crust - A consolidated undrained triaxial test from URS Boring 2F-01-29 was chosen to evaluate hyperbolic parameters for the upper desiccated fine grained soil modeled in cross section at Station 230+00. The boring was performed at the landside field area of the existing levee. This test was chosen, as the soil description and soil properties are consistent in description, depth, plasticity, and blow counts to samples taken at or near Station 230+00. Strength testing values also correlate with other samples tested in the upper native soils in the area. A consolidation test is also available for the sample. The initial parameters chosen were an Rf of 0.67, K-Modulus of 1400, and an n-exponent of 2.7 (limited to 1.0 in SIGMA/W).

Upper Soft Soil – Various soft soil specific testing (strength, permeability, and consolidation) was performed on samples taken from the northern portion of the SREL site, specifically between Station 0+00 and 190+00 (SREL1). Soft soils are continuous through the SREL site and are classified similarly to the soft soils at Station near 230+00, so these tests are

thought to be representative of the soft soils throughout the project. An Osterburg sampler was required to be used in order to obtain samples in the soft material. A consolidated undrained test performed on a sample taken at an approximate depth of 10-13 feet below the surface at the levee toe near Station 188+00. This test was used over the others because the description of the material was most similar in description to the soft soil material near Station 230+00. Hyperbolic parameters were determined from the test data. The initial parameters were 0.92 for Rf, 0.45 for the n exponent, and 750 for the K-Modulus. The hyperbolic parameters proved to be a good fit with the testing data.

Lower Soft Soil – The soft soil underneath the existing levee was the same material seen in borings near the landside levee toe and field areas. One difference was that the blow counts were higher in the crown borings versus the landside toe and field borings. This difference is thought to be attributed to the fact that the soils beneath the levee were consolidated under the weight of the existing levee. The initial parameters were 0.92 for Rf, 0.45 for the n exponent, and 750 for the K-Modulus, which were the same as the parameters for the Soft Soil 2. The parameters were then adjusted to more accurately match the behavior in the field. The final parameters used are shown in Table 3-1.

Firm Sandy Clay - The material beneath the soft soils were stiff and were modeled with a linear elastic model using a large modulus of elasticity, as shown in the Table 3-1 below. Since little deformation was seen in the inclinometer section embedded in this material and laboratory tests were not performed on this material, the modulus was set very high as to not impact its influence on the results of the upper layers of soil. It is also recommended by the literature that modeling an excavation with finite elements that the mesh should end in a relatively hard material (Kulhawy, 1977).

Table 3-1: Summary of Parameters Used

Parameter	Sand Fill	Clay Fill	Desiccated Crust	Upper Soft Soil	Lower Soft Soil	Firm Sandy Clay	Soil Bentonite
Total Unit Weight (lb/ft^3)	110	123	114	113	120	115	80
Poisson's Ratio	0.36	0.35	0.25	0.34	0.34	0.4	0.32
K_o	0.8	3	1	0.65	0.65	0.67	0.47
Hyperbolic Model Parameters							
Cohesion (lb/ft^2)	0	100	50	50	50		0
Friction Angle (degrees)	38	27	27	34	34		32
R_f	0.85	0.98	0.88	0.92	0.60		
K	1400	1300	1500	1100	1200		
n	0.36	0.89	0.67	0.45	0.45		
Linear Elastic Model Parameters							
E' (lb/ft^2)	*	*	*	*	*	20,000,000	
Cam Clay Model Parameters							
OCR							1.00
κ							0.0049
λ							0.07
e_o							1.0
Hydraulic Conductivity (ft/day)	2.8	0.112	0.28	0.0112	0.0112	0.28	0.00028

*Estimated from hyperbolic curve

3.5 Description of Finite Element Model

Elements were established by meshing with 8-noded quads and 3-noded triangles at a global size of 3 feet. A smaller spacing was used near the slurry wall and fill areas. Levee fill and the native alluvial soil layering used in the model was simplified as shown in Figure 3-4.

3.6 Procedures for Modeling the Construction Sequence

The model was divided into steps based on the actual construction sequence. All steps were modeled with boundary conditions on the bottom and sides of the model. On the left and right side of the model the soil was constrained in the x direction and at the bottom of the model the soil fixed in the x and y directions. The bottom, left, and right edges were spaced a distance from the area of study in the model where these conditions would not have an effect on the area of interest.

Unless otherwise noted, the linear elastic method was used for the soil models. The rationale for using this method was to be able to use effective stress parameters with pore water pressure changes. Also another advantage was to evaluate the time-rate of consolidation of the soil bentonite fill with lateral movement. When the linear elastic model is used the hydraulic conductivity of the soils can be applied and the model can be run over a specified period of time. As mentioned, hyperbolic parameters were used to estimate the Effective Modulus of the linear elastic model. This is thought to be acceptable modeling practice as the soils at the site did not reach a plastic condition; in other words the soil does not go beyond the initial portion of the hyperbolic curve.

The first step was an in-situ analysis, also known as the gravity turn-on analysis. The in-situ analysis was conducted prior to modeling fill and trench construction to establish horizontal and vertical in-situ stresses based on the material unit weight, depth, and K_o values. The following three steps modeled the filling of the working platform and stability berm on the landside of the existing levee from and elevation of about 26 feet to an elevation of 35 feet and 30-34 feet respectively. The filling of the working platform was modeled in SIGMA/W with a load deformation analysis.

Performed with a coupled stress-pore water pressure analysis, the next step was the excavation of the sixty-foot deep wall and concurrent filling of the excavation with the bentonite slurry fluid. This step was modeled by removing the materials assigned to the regions in the area of the trench and applying a stress distribution along the sides and bottom of the trench; modeled as the unit weight of the slurry times the depth of the excavation. This was determined to be an acceptable procedure, as slurry is fluid and has no shear strength. Field testing on the slurry mixture indicates that the slurry material density was about 75 pcf when placed into the trench. Due to the nature of the construction, mixing with soil from the trench excavation occurred and soil particles were suspended in the slurry mixture. Based on test results, the in place density was tested again and varied from about 75-85 pcf. An average value of 80 pcf was used for the stress distribution. Part of the excavation was below the water table and was adjusted in the model to the fact that slurry is relatively impermeable. The excavation was modeled as drawndown below the wall, but was reestablished on the landside of the wall to keep the model symmetrical. Any possible differential water pressure was assumed to be negligible.

Finally, the addition soil-bentonite fill was modeled. Soil bentonite material properties were assigned to the regions in the trench. Due to the consolidation properties of the soil bentonite fill, a Cam Clay model was chosen to represent the soil-bentonite fill material; parameters were selected based on Filz and Baxter (2007) and are included in the summary table above. Table 3-2 below shows the steps modeled with SIGMA/W and the range and direction of recorded and modeled lateral deformation values in the soft material.

Table 3-2: Summary of Steps Used in FEM Model

Construction Step Modeled	Step Number	Time assigned to each step	Type of Analysis
Initial Stresses Assigned	1	N/A	Load Deformation
Fill Placement/Surcharge	2-3	N/A	Load Deformation
Excavation of trench under bentonite slurry	4	3 days	Coupled Stresses/Porewater Pressure
Backfill trench/consolidation	5	21 days	Coupled Stresses/Porewater Pressure

In the following chapter the results of the horizontal displacement values obtained in the model are compared with the measured displacement in the inclinometers. Further analysis was performed to revise and refine the model. The material properties are adjusted and discussed, as to how they impacted the model results.

CHAPTER 4: RESULTS AND DISCUSSION

4.1 Introduction

In this chapter a comparison of the model results and the inclinometer data are discussed. In order to better understand what parameters were the most influential in the analysis, a sensitivity analysis was performed. It was also of interest to see what parameters could be adjusted to obtain a better fit to the inclinometer data. The initial and revised analysis and influence of the material parameters adjusted and their impact on the model are discussed below. Based on the results of all the analyses insight is given into the mechanisms that are crucial to understanding the lateral deformation behavior observed in the SREL inclinometers during the construction of the SB wall.

4.2 Initial Results -Comparison of Measured and Modeled Deformation

The results of the lateral deformation during the excavation and subsequent filling were compared with the construction platform inclinometer readings.   The two inclinometers, SREL5A-230-R1 and SREL5A-231-T1 were used to compare the results of the finite element model. SREL5A-230-R1 was located seven feet from the SB wall trench construction. Data from SREL5A-230-R1 used to compare the lateral deformation obtained from the finite element model results to the excavation phase as well as the backfilling phase of the SB wall construction. SREL5A-231-T1 was located 100 feet away from the trench. The data from this inclinometer was used for the backfilling portion of the wall only, as readings were not taken during the excavation portion of the construction. Figures 4-1 and 4-2 show the results of the finite element analysis compared to the inclinometer data for both inclinometers.
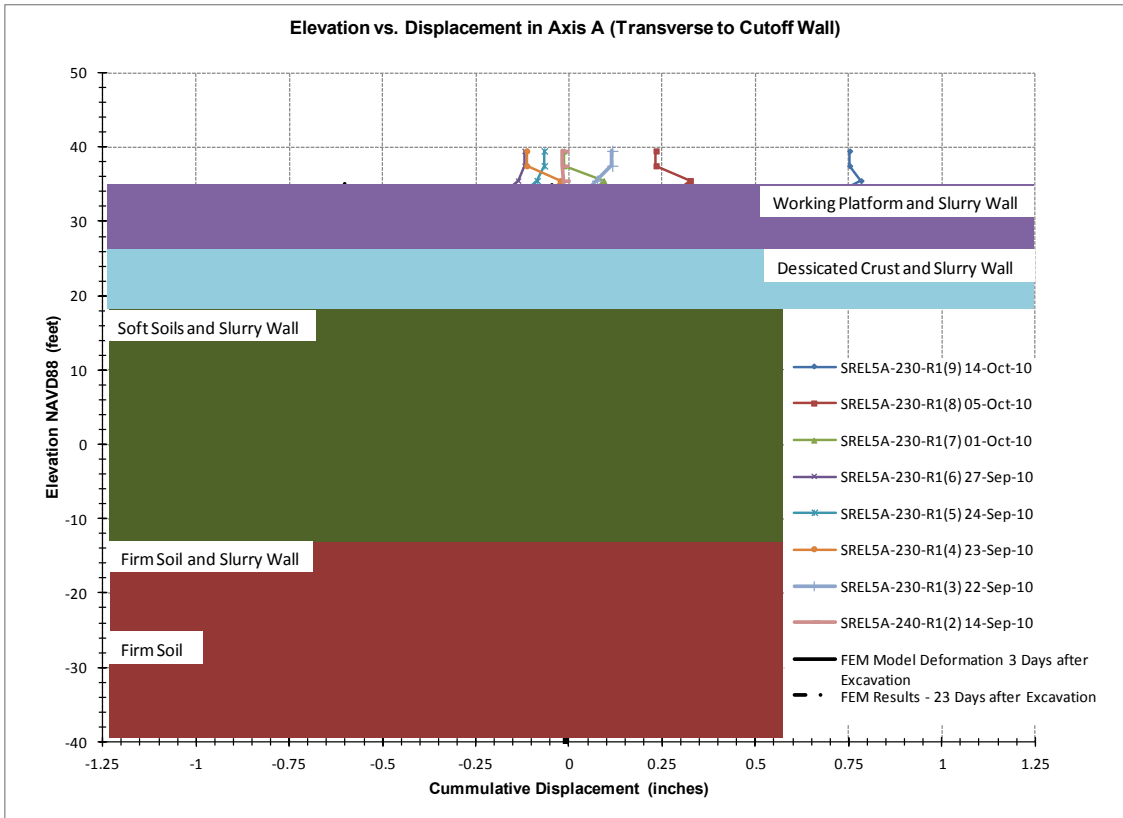
Figure 4-1: Comparison of Finite Element Results with Inclinometer Data at SREL5A-230-R1
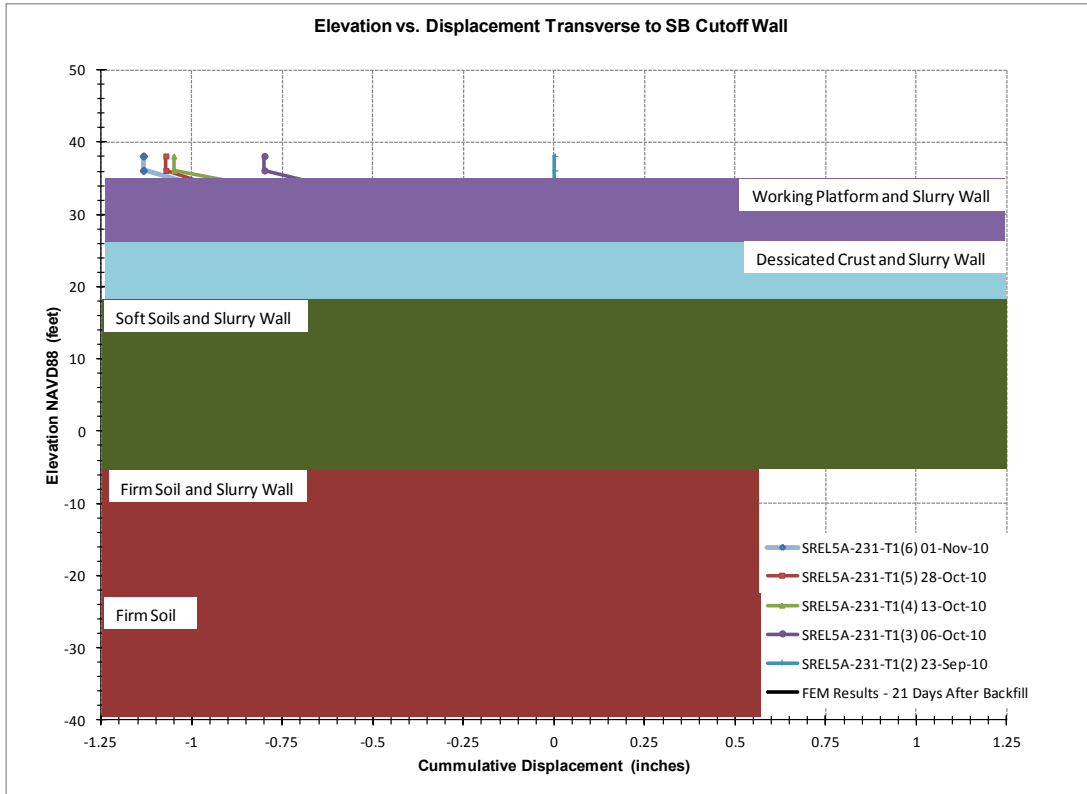
Figure 4-2:Comparison of Finite Element Results with Inclinometer Data at SREL5A-231-T1

Results from the finite element analysis were compared with the inclinometer results at two separate steps during the construction: before backfilling of the trench occurred (after step 4) and 21 days after backfilling occurred (after step 5). It is important to note that negative displacement is away from the trench in SREL5A-230-R1 and toward the trench in SREL5A-230-T1 due to the placement of the inclinometers, shown in Figure 3-1. Also, the upper eight feet of SREL5A-231-T1 were above ground at the time of the excavation and backfilling, so no results were calculated in the finite element analysis. This instrument was also in a path of construction equipment, so some of the movement near the top of the inclinometer may have been influenced by construction activities.

As can be seen from the results above, good agreement is achieved between the finite element analysis results and the inclinometer data. Both the finite element analysis and the inclinometers show that the maximum lateral deformations occur in the soft soils, below the fill and desiccated crust, and then decrease with depth. The trend of the movement away from the trench after the excavation and before the fill, as well as the movement toward the trench after backfilling is shown by both the inclinometers and the finite element modeling. The maximum lateral movement recorded in the finite element model before the bentonite fill was placed was 0.78 inches in the soft soils, and a value of 0.61 inches was recorded in the inclinometers in the soft soils. At 23 days after the excavation the inclinometer recorded 0.88 and 0.60 inches of movement for the platform and the toe inclinometer respectively at the surface. The finite element model predicted a maximum 0.55 inch and 0.20 inches of movement respectively, both in the upper layer of soil. The maximum value in the toe inclinometer was taken from the top, as discussed this inclinometer was likely impacted by construction activities. A better comparison would be to evaluate the deeper layers in which case the difference between the inclinometer and model deformations are in better agreement.

The model overestimates the deformation in the lower soft soil layer in step 4. The model overestimates the lateral deformation in the upper soft soils in the toe inclinometer 21 days after the excavation.

4.3 Model Calibration

Changes in material parameters and cross section geometry were analyzed in an effort to obtain a better fit to the inclinometer data, specifically if the location of the maximum deformation in the model could better fit the inclinometer results in step 4 and if a better fit could be obtained between the model and toe inclinometer data in step 5. Adjustments were made to

the model and material parameters were adjusted. Some of the material parameters that were

adjusted were realistic and better matched the parameters found in the constitutive models. Other

parameters were adjusted and deemed unreasonable and not used.

In order to obtain the initial finite element results, shown in Figures 4-1 and 4-2, the K-

modulus, which dictates the stiffness of the soil, had to be increased from the values determined

from the constitutive models. Table 4-1 shows the adjustment made for each layer from the

values determined by the test.

Table 4-1: Comparison of K-modulus Values Predicted versus Analysis

Soil Layer	Sand Fill	Clay Fill	Desiccated Crust	Upper Soft Soil	Lower Soft Soil
K-modulus predicted from constitutive model	1400	1000	1400	750	750
K-modulus used for initial results	1400	1300	1500	1100	1200
K-modulus used in calibrated results	1400	1000	1400	750	1000

The K-modulus values used in the model were compared with typical values in for

undrained tests in Table 6 of Duncan et al. (1980). The values in the model seemed unreasonably

high compared to the typical values for silts and clays in Duncan et al. (1980). Another

observation while performing the initial analysis was that no matter how much the parameters

were adjusted, the soft soils were showing approximately the same amount of displacement as

the upper layers, which was not seen in the SREL5A-230-R1 inclinometer. It was thought that

this was occurring because SIGMA/W solves for continuity in terms of displacement and then
calculates the stresses and strains. In order to break this continuity between the upper soils and
lower soils an interface layer was applied below the clay fill layer in the form of a slip surface.
The slip surface was given the values shown in Table 4-2.

Table 4-2: Summary of Slip Surface Parameters

Slip Surface Parameters	Cohesion (lb/ft^2)	Friction Angle	Shear Modulus (lb/ft^2)	Unit Weight (lbs/ft^3)	Poisson's Ratio
	50	27°	750,000	114	0.25

In order to initiate the slip surface a certain amount of displacement must occur
following Equation 2 below.

$$\Delta d = 2F/LG \qquad\qquad\qquad (2)$$

Where:

d = displacement

F = Force

L = Length

G = Shear Modulus

Interface values were chosen based on the properties of the desiccated crust. The shear
modulus was determined based on the best fit between the inclinometer and finite element data
after K-modulus values were reset to the values determined from the testing (Table 4-1), as the
values determined from the testing were considered reasonable and fit the test data well. After a
good fit was determined material parameters were adjusted to try to refine the data further.

The hydraulic conductivity of the soils was thought to be conservative, as the values used were based on established values for the SREL levee seepage analysis performed by Kleinfelder (2008). In the case of an undrained condition, it was thought less deformation might occur. After decreasing the hydraulic conductivity of the soft soils by two orders of magnitude, a significant reduction in deformation did not occur during any of the steps 4 and 5 of the analysis.

Adjustments were made in the K_o values. Reducing the K_o values of the soils decreased the lateral deformation during the excavation step, but did not influence the movement during the backfilling step. Ultimately the K_o values were not changed, as the initial values were reasonable and adjustments needed to make an impact in the deformation made the values vary to much from the initial values calculated from Mayne and Kulhawy (1982).

During the initial analysis a stiffer response during excavation and backfilling was required in order to better match the inclinometer data. The R_f parameter also had an influence on the stiffness. Increasing the values produced a slightly stiffer response. Like the K-modulus, the R_f parameter was also calculated from the CU tests performed on the soils. Altering this value enough to create a stiffer response was not realistic based on Duncan et al. (1980).

Adjusting the soil stratigraphy was also performed to see if it had an influence on the finite element model. One example is the soils in the model were adjusted in that the soft soils under the existing levee were modeled as stiffer, more consolidated versus the soils in the area of the cutoff wall excavation. The upper and lower soft soil layers were combined and the soft soils under the levee were reclassified as consolidated soft soil and the soil in the area of the cutoff wall was classified as a less consolidated material. Figure 4-3 shows the adjusted soil geometry. The less consolidated material was assigned the parameters assigned to the upper soft soil and

the consolidated soil under the existing levee was given similar parameters similar to the lower soft soil.
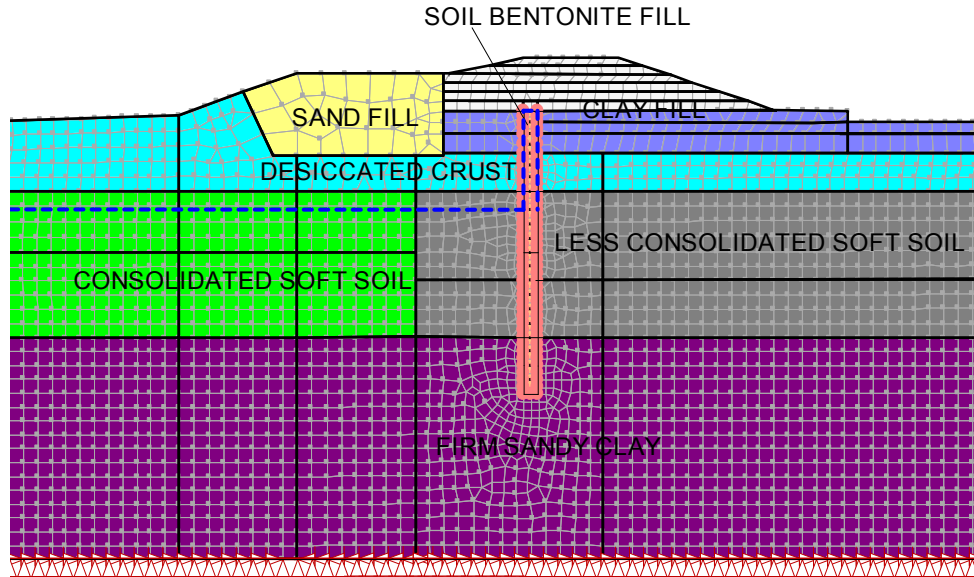
Figure 4-3: Soil Stratigraphy Changes in Calibrated Model

Other configurations attempted were decreasing the thickness of the desiccated crust and increasing the thickness of the firm sandy clay. All of the results obtained from the soil layer adjustments resulted in negligible change from the original stratigraphy and therefore were not used in the final results.

The final adjusted results of the finite element model versus the inclinometer are presented in Figure 4-4 and 4-5 below.
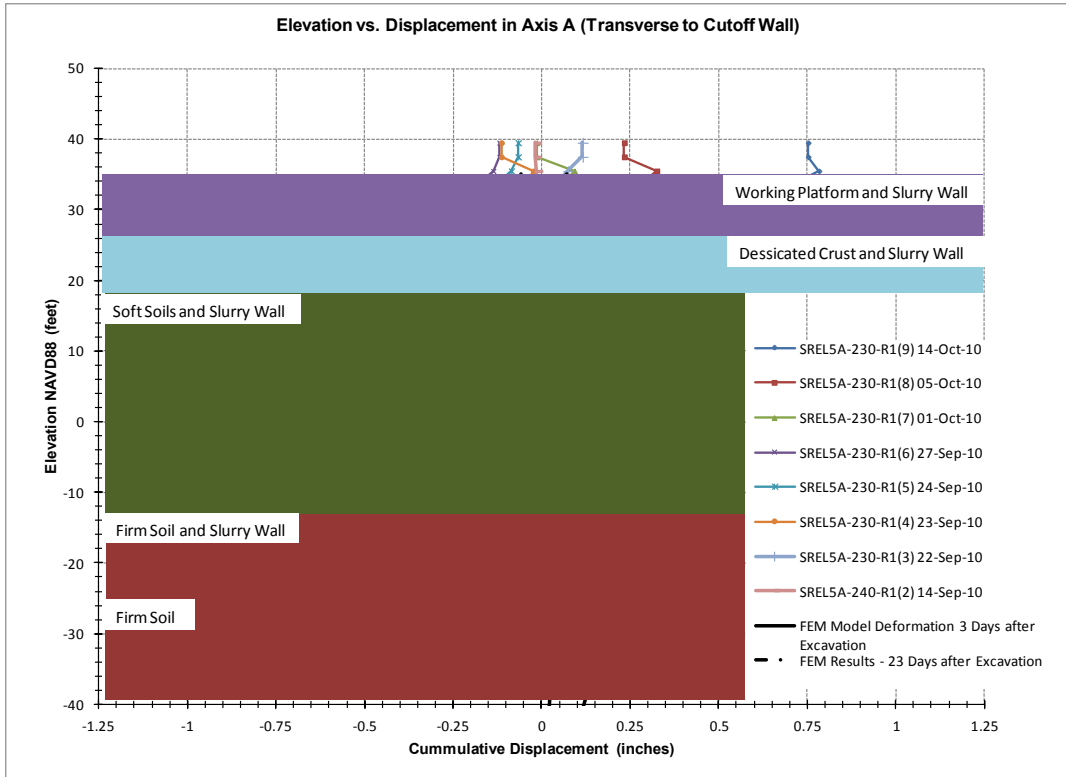
Figure 4-4: Comparison of Finite Element Results with Inclinometer Data after Calibration at SREL5A-230-R1
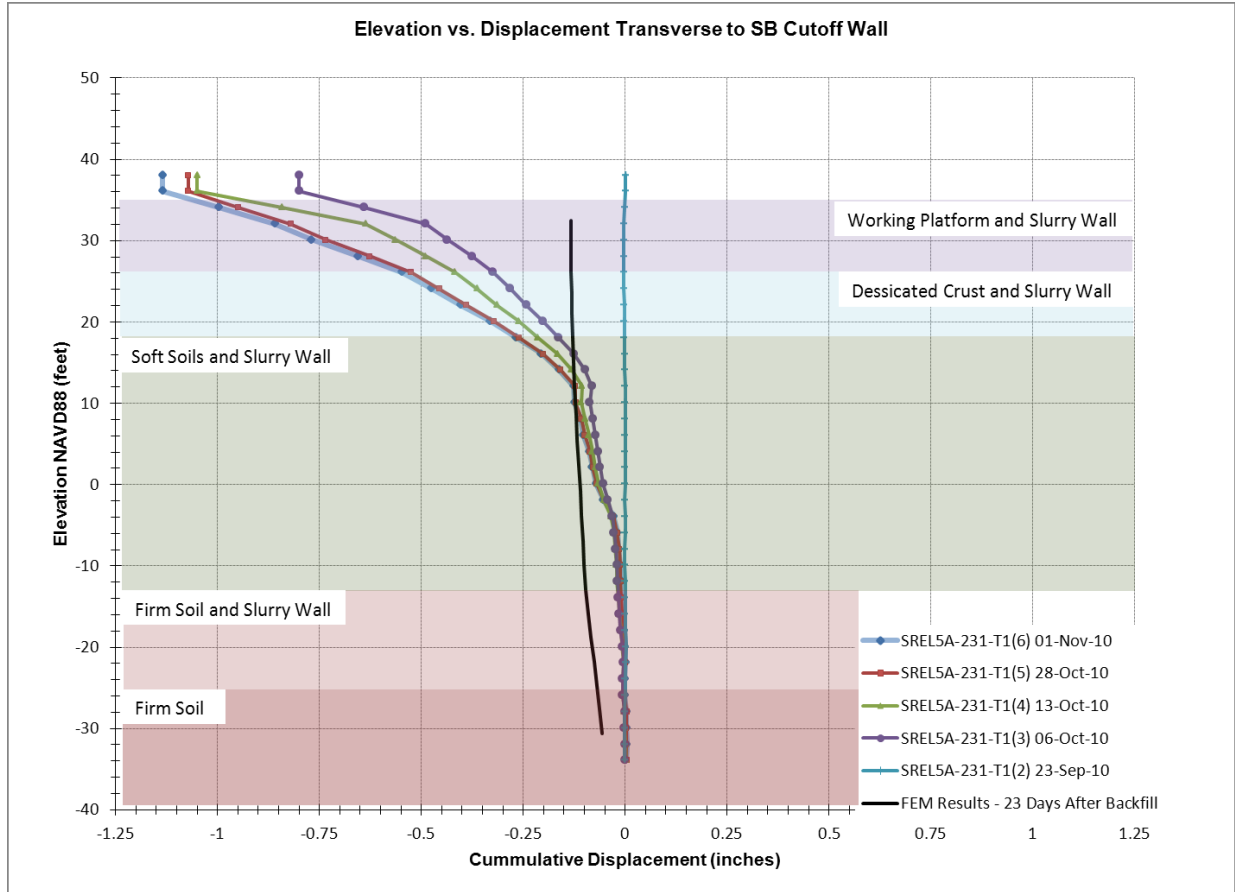
Figure 4-5: Comparison of Finite Element Results with Inclinometer Data after Calibration at SREL5A-231-T1

As can be seen from the calibrated results, a curve that better fits the inclinometer data is achieved in the calibrated finite element analysis results. The maximum lateral movement recorded in the finite element model before the bentonite fill was placed was 0.62 inches in the soft soils, and a value of 0.61 inches was recorded in the inclinometers in the soft soils. At 23 days after the excavation the inclinometer recorded 0.88 and 0.60 inches of movement for the platform and the toe inclinometer respectively at the surface. The finite element model predicted a maximum 0.30 inch and 0.15 inches of movement respectively, both in the soft soils. When a comparison is made between the maximum movement in the soft soils and firmer soils for the consolidation, a better agreement in achieved, as can be seen in Figures 4-4 and 4-5.

An attempt was made, as discussed above, by modifying the material parameters, to adjust the location of the maximum deformation. Little impact was made that kept material parameters in a reasonable range.

4.4 Evaluation of Lateral Deformation

The observed pattern of cutoff wall trench deformations can be possibly explained by considering the horizontal stress field near the slurry trench. Prior to excavation, the loose silts may have had a horizontal pressure between the active pressure and at rest pressure. Assuming a total unit weight of 110 pcf and a friction angle of 34 degrees, $K_o = 1 - \sin \phi = 0.44$ and $Ka = (1+\sin\phi)/(1-\sin\phi) = 0.28$. The effective horizontal stress increment would be $\Delta\sigma'_h = (K_a \text{ to } K_o)^* \gamma_{sub} = 13$ to 21 pcf. Upon excavation of the slurry trench, the trench is supported by water-soil-bentonite slurry with an effective density in excess of $80 - 62 \text{ pcf} = 18$ pcf. While backfill is being placed and is still fluid, it typically has an effective density of around $125 - 62 \text{ pcf} = 63$ pcf. The apparent pressure of the slurry trench at each step in construction equals or exceeds the preceding in situ horizontal pressures. Only when the backfill stops being a fluid (due to lack of shearing due to trench backfilling and sufficient initial reduction in pore pressures to gain some strength) will the horizontal stresses be reduced $\Delta\sigma'_h = K_a * \gamma_{sub} = 18$ pcf.

The majority of the movements toward the wall resulted after the slurry trench was no longer fluid and was consolidating. Since movement toward the slurry wall were observed for several weeks in most instances, the additional horizontal movements after completion of filling and apparent solidification of the backfill are hypothesized to result primarily from horizontal consolidation of the slurry backfill. Typical soil-bentonite backfill properties were a dry unit weight of 98 pcf, initial water content of 28 percent and 40 to 80 percent fines. Based on

consolidation tests for project backfill, the backfill should experience 5 to 12 percent

consolidation strain, or 1 to 4 inches of lateral movement at top and bottom, respectively, for a 3-foot-thick cutoff wall if all consolidation were accommodated laterally. The actual distribution

and magnitude of lateral consolidation would be dependent on the continuity and shape of any

soil wedge deformation of the adjacent native soils.

Laboratory time rate of consolidation for backfill was approximately 8 square feet per

year. Based on these parameters, a 3-foot-wide slurry wall controlled by double-sided drainage

should be 50 percent consolidated at 3 weeks and 90 percent consolidated at 12 weeks. This

duration is roughly consistent with the continuation of lateral movements observed for the SREL

cutoff wall.

Figure 4-6 shows a comparison between inclinometer deflections and trench backfill

settlements as a function of time. Settlement points consisted of a plywood platform installed on

the trench backfill with a pipe riser extending above the temporary soil cover to allow survey

readings. The settlement points were installed shortly after the trench backfill was completed.

These settlement points allowed monitoring to confirm that backfill settlement was at a slow rate

before permanent cap construction, to ensure that a horizontal gap or void would not occur at the

top of the slurry wall after adjacent levee completion. The pattern and rate of reduction of

settlements and lateral movements is comparable to the shape of the theoretical time-rate

settlement curve computed for a 3-foot-thick consolidating layer, i.e. the width of the trench.

Figure 4-6 suggests that slurry wall consolidation was approximately 50 percent complete when

the working platform inclinometer and settlement sensors were removed at about 3 weeks after

completion of backfill.
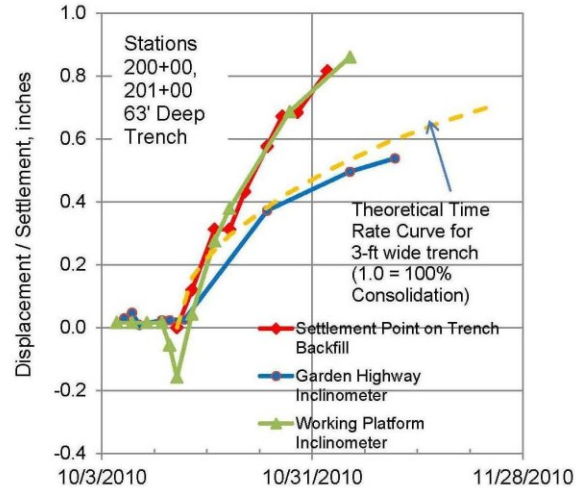
Figure 4-6: Comparison between Inclinometer Deflections and Trench Backfill Settlement Measurements versus Time

The description of the modes of deformation described above fit with what was determined by the finite element analysis. In step 4, finite element results were impacted by the material properties, specifically the stiffness of the soil layers. Whereas in step 5, although stiffness did have some impact relative to the movement in step 4, the movement occurred more uniformly across all soil layers, and related to the consolidation of the backfill material assigned to the trench.

CHAPTER 5: CONCLUSIONS

The importance of improving the levee systems surrounding Sacramento, California has been elevated since Hurricane Katrina. The heightened awareness produced a sense of urgency to repair the failing levees. One of the levees that went through vital upgrades was the SREL levee, just north of the city. During the construction of soil-bentonite slurry walls on the levee unexpected lateral movements were recorded by inclinometers. In order to evaluate the lateral movements, a finite element model of a soil-bentonite cutoff wall was developed in this thesis to replicate the construction process of a soil-bentonite slurry wall constructed in the SREL levee.

Case studies of the deformation of soil-bentonite cutoff walls were discussed in order to try to better understand the construction process and soil deformation behavior. Also, previous examples of finite element modeling of soil-bentonite cutoff walls were presented. The examples were found to be limited and the technology used to produce them has been updated significantly since their time. Due to the advances, it become more feasible for today's geotechnical engineer to use and evaluate a finite element analysis program.

A finite element analysis program was used to model a cross section of the SREL levee. The construction in the model was set-up in several steps to simulate a staged analysis, as discussed in the case history. To model the site conditions, geotechnical data were compiled from laboratory tests, field tests, and in-situ tests. From this data, a soil profile was created and constitutive models were developed from laboratory testing performed on local samples. SIGMA/W was used for the analysis. Fully coupled fluid flow and deformation analyses were used. Ultimately a linear-elastic model was used with the modulus based on parameters from the

development of the Duncan and Chang (1970) hyperbolic model. A modified Cam Clay model was used for the soil-bentonite fill material based on Filtz and Baxter (2007).

The excavation step was modeled by removing the elements in the trench and applying stress distributions to the trench wall and trench bottom to represent the bentonite-water slurry pressure. The backfilling step was modeled by assigning the soil-bentonite properties to the area in the model, previously removed in the excavation step. After backfilling, the initial excess pore pressures in the soil-bentonite were allowed to dissipate over time, which was modeling the consolidation of the soil-bentonite.

With some adjustments to the parameters the lateral deformation results determined by the finite element model proved to fit the inclinometer data within reason. The model was then adjusted to determine the sensitivity of various parameters. It was calibrated in an attempt to fit in inclinometer trends as well. The following changes were made during calibration. The K-modulus was reduced to better fit the laboratory data and an interface layer was applied between the boundary of the clay fill and the desiccated crust. Both of these changes resulted in a better fit to the data compiled from the inclinometer.

It was thought that the fact that SIGMA/W calculates continuity in terms of displacement could be causing some of the variation seen between the actual results and the finite element model. In order to get more accurate results, interface layers would need to be applied to the border between layers. This seems unpractical for modeling purposes, as little information is known about the frictional properties between each of the layers. Also, it is important to note that the model is greatly simplified. It is likely the soil stratigraphy varies

greatly in all directions. A finite element model is meant to give an estimate and for this thesis that goal is met.

One of the most important lessons from performing this analysis is that the background knowledge of soil mechanics is important along with how the computer program is using the data that it is entered into it. While a program like SIGMA/W has a lot of processing power making modeling available to the working engineer, good engineering judgement is still necessary.

REFERENCES

ASCE (2013) "2013 Report Card on America's Infastructue," Levees. ASCE. Accessed on May 25, 2013. http://www.infrastructurereportcard.org/levees/

Barrier Containment Technologies or Environmental Remedial Applications. (1995). John Wiley & Sons, Inc. R.R. Rumer and M.E. Ryan eds., New York.

Baxter, Diane Y. and Filtz, George M. (2007) "Deformation Predictions of Ground Adjacent to Soil-Bentonite Cutoff Walls using the Finite Element Method." ASCE Conference Proceedings of Sessions of Geo-Denver 2007

Baxter, D.Y. (2000). "Mechanical behavior of soil-bentonite cutoff walls." Ph.D. dissertation, Virginia Polytechnic Institute and State University, Blacksburg, VA.

Bentler, D.H., Morrison, C.S, Esterhuizen, J.J.B., and Duncan, J.M. (1998). "SAGE User's Guide: A Finite Element Program or Static Analysis of Geotechnical Engineering Problems." Version 2.03, The Charles E. Via Jr. Department of Civil Engineering, Virginia Tech, Blacksburg, VA.

Clark, I.H. (1994). Modeling of soil-bentonite cut off wall." Proceedings ANCOLD Conference on Dams, Tasmania.

D' Appolonia, D.J. (1980). "Soil-Bentonite Slurry Trench Cutoffs." *Journal of Geotechnical Engineering*, ASCE, 106(4), 399-417

Duncan, J.M. and Chang, C.Y. (1970). "Non-Linear Analysis of Stress and Strain in Soils." *Journal of the Soil Mechanics and Foundation Division*, ASCE, Vol. 96 No. SM5, 1629-1653

Duncan et al (1980). "Strength, Stress-Strain and Bulk Modulus Parameters for Finite Element of Stresses and Movements in Soil Masses." Geotechnical Engineering Report, No. UCB/GT/08-01, University of California, Berkeley California.

Filt, G.M., Boyer, R.D, and Davidson, R.R. (1997). "Bentonite-water slurry rheology and cutoff wall trench stability." In situ Remediation of the Geoenvironment, GSP No.71, ASCE, Reston, VA, 121-139

Filtz, G.M., Baxter, D.Y., Bentler, D.J., and Davidson, R.R. (1999). "Ground Deformation Adjacent to a Soil-Bentonite Cutoff Wall." Geo-Engineering for Underground Facilities, GSP No. 90, ASCE, Reston, VA, 121-139.

Geo-Slope International, Ltc, (2007). Computer Software, Version 7.21

Helley, E.J., and Harwood, D.S. (1985), "Geologic Map of the Late Cenozoic Deposits of the Sacramento Valley and Northern Sierran Foothills, California," U.S. Geological Survey Miscellaneous Field Studies Map MF-1790.

Khoury, M.A., Fayad, P.H., and Ladd, R.S. (1992). "Design, Construction, and Performance of a Soil-Bentonite Cutoff Wall Constructed in Two Stages." *Slurry Walls: Design, Construction and Quality Control*, ASTM STP 1129, D.B. Paul, R.R.

Kleinfelder (2010) "Geotechnical Basis of Design Report, Sacramento River East Levee, SREL 2 (Reaches 5 through 9), Natomas Levee Improvement Program, Sacramento and Sutter Counties, California," Kleinfelder Project 94582, for Sacramento Area Flood Control Agency, Sacramento, CA.

Kleinfelder (2010a) "Geotechnical Basis of Design Report, Report Supplement, Sacramento River East Levee, SREL 2 (Reaches 5 through 9), Natomas Levee Improvement Program, Sacramento and Sutter Counties, California," Kleinfelder Project 94582, for Sacramento Area Flood Control Agency, Sacramento, CA.

Kleinfelder, (2010b). "Supplemental Studies – Soft Foundation Soils, Sacrameto River East Levees, SREL 1 and 1B (Reaches 1 through 4B), Natomas Levee Improvement Program, Sacramento and Sutter Counties, California," Kleinfelder Project 98145, for Sacramento Area Flood Control Agency, Sacramento, CA.

Kulhawy, F.H. and Mayne, P.W. (1990), Manual on Estimating Soil Properties or Foundation Design, Electrical Power Research Institute EPRI EL-6800, Palo Alto California.

Pease, Jonathan W. and Nardi, Christopher R., (2012). "Levee cutoff wall design and construction through loose Sacramento River silts." Proceedings of the USSD 2012 Annual Meeting and Conference, New Orleans, LA.

Petroski, Henry (2006). "Levees and Other Raised Ground." 94, American Scientist, pp.7-11.

Weisner, Matt and Reese, Phillip (2012). "What if a Superstorm Strikes Sacramento? Flooding Danger Puts the Capital at Risk of a Disaster Worse than Sandy." Sacramento Bee. November 18, 2012. Accessed on May 30, 2013. http://www.sacbee.com/2012/11/18/4994108/what-if-a-superstorm-strikes-sacramento.html

SAFCA (2008) "The Sacramento Area Flood Control Agency" Sacramento Area Flood History. Accessed June 1, 2013. www.safca.org/history.html

USACE (2000), "Design and Construction of Levees," US Army Corps of Engineers Engineering Manual EM 1110-2-1913, dated April 30, 2000.

USACE (2005), "Design Guidance for Levee Underseepage," US Army Corps of Engineers Technical Letter ETL 1110-2-569, dated May 1, 2005.

Xanthakos, P.P. (1994). Slurry Walls as Structural Systems, 2nd Ed, McGraw-Hill, New York.

APPENDIX

Constitutive Modeling Results

Soil: Fill Material   Borrow Site 2A

Confining Pressures		Data for Deviatoric Modulus Parameters						
		70% Stress Level				95% Stress Level		
σ_3	$(\sigma_1-\sigma_3)_f$	$\sigma_1-\sigma_3$	ε_a	$\varepsilon_a/(\sigma_1-\sigma_3)$		$\sigma_1-\sigma_3$	ε_a	$\varepsilon_a/(\sigma_1-\sigma_3)$
288	966	676.2	0.0014	2.07E-06		917.7	0.0224	2.44E-05
806	1769	1238.3	0.0015	1.21E-06		1680.6	0.012	7.14E-06
1765	3323	2326.1	0.009	3.87E-06		3156.9	0.0311	9.85E-06

P_a=   2116   psf

σ_3/P_a	$1/(\sigma_1-\sigma_3)_{ult}$	R_f	E_i/P_a
0.1	1.06E-03	1.03	813
0.4	5.65E-04	1.00	1297
0.8	2.71E-04	0.90	330

R_f Average= 0.98

Raw Test Data
Confining
Pressures
Sigma 3

psf	Pa (psf)	Sigma3/Pa
288	2116	0.13610586
806	2116	0.380907372
1765	2116	0.834120983

Sigma 3 = 288 psf	Axial Strain	Deviator Stress	Sigma 3 = 806 psf	Axial Strain	Deviator Stress	Sigma 3 = 1765 psf	Axial Strain	Deviator Stress
	0.00	84		0.00	137		0.00	48
	0.10	614		0.10	960		0.10	1162
	0.20	812		0.20	1255		0.20	1397
	0.30	877		0.30	1353		0.31	1160
	0.42	942		0.40	1417		0.41	1159
	0.51	974		0.50	1481		0.51	1124
	0.61	973		0.60	1545		0.62	1660
	0.71	1038		0.71	1544		0.72	1826
	0.81	1037		0.81	1542		0.82	1891
	0.91	1036		0.91	1540		0.92	1956
	1.03	1002		1.01	1571		1.03	2055
	1.13	1033		1.11	1635		1.13	2119
	1.23	1032		1.21	1633		1.23	2151
	1.33	999		1.31	1697		1.33	2215
	1.42	998		1.41	1695		1.44	2213
	1.54	996		1.51	1629		1.53	2277
	1.64	995		1.61	1692		1.64	2308
	1.74	962		1.71	1690		1.74	2372
	1.84	993		1.81	1656		1.85	2403
	1.94	992		1.91	1719		1.95	2433
	2.06	959		2.01	1685		2.05	2464
	2.16	958		2.12	1683		2.15	2528
	2.26	989		2.21	1681		2.26	2492

2.35	956	2.31	1647	2.36	2522
2.45	955	2.41	1678	2.46	2552
2.57	986	2.52	1676	2.56	2583
2.67	1017	2.62	1674	2.67	2646
2.77	984	2.72	1673	2.77	2643
2.87	983	2.82	1671	2.87	2673
2.97	982	2.92	1669	2.97	2670
3.09	981	3.02	1667	3.08	2700
3.18	1012	3.12	1666	3.18	2763
3.28	1011	3.22	1664	3.28	2760
3.38	1010	3.32	1630	3.38	2790
3.48	1009	3.42	1661	3.49	2787
3.60	1008	3.52	1691	3.59	2784
3.70	1007	3.62	1721	3.69	2846
3.80	1006	3.72	1719	3.79	2843
3.90	1005	3.82	1654	3.90	2840
4.00	1003	3.93	1684	4.00	2869
4.11	970	4.03	1713	4.10	2899
4.21	969	4.13	1712	4.20	2863
4.31	968	4.23	1710	4.31	2892
4.41	999	4.33	1676	4.41	2889
4.51	966	4.43	1738	4.51	2918
4.63	997	4.53	1736	4.61	2915
4.73	964	4.63	1703	4.72	2944
4.83	963	4.73	1764	4.82	2973
4.93	962	4.83	1699	4.92	3002
5.02	961	4.93	1760	5.02	2999
5.14	929	5.03	1727	5.13	3028
5.24	928	5.13	1725	5.23	3025
5.34	927	5.23	1692	5.34	3053
5.44	926	5.34	1721	5.43	3050
5.54	925	5.44	1782	5.54	3047
5.66	924	5.53	1687	5.64	3075
5.76	923	5.64	1747	5.74	3072
5.86	922	5.74	1714	5.85	3069
5.95	921	5.84	1712	5.95	3097

6.05	920	5.94	1710	6.05	3094
6.15	919	6.04	1709	6.15	3090
6.27	918	6.14	1707	6.26	3119
6.37	917	6.24	1736	6.36	3084
6.47	916	6.34	1765	6.46	3080
6.57	915	6.44	1763	6.56	3077
6.67	914	6.54	1730	6.67	3105
6.79	912	6.64	1728	6.77	3102
6.88	912	6.74	1757	6.87	3098
6.98	911	6.84	1755	6.98	3126
7.08	910	6.95	1753	7.07	3154
7.18	909	7.05	1751	7.18	3151
7.30	938	7.15	1750	7.28	3210
7.40	968	7.25	1748	7.38	3206
7.50	967	7.35	1746	7.48	3203
7.60	966	7.45	1744	7.59	3199
7.70	965	7.55	1742	7.69	3227
7.81	964	7.65	1771	7.79	3254
7.91	963	7.75	1769	7.90	3251
8.01	992	7.85	1828	8.00	3278
8.11	960	7.95	1795	8.10	3275
8.21	990	8.05	1793	8.21	3271
8.33	958	8.15	1761	8.31	3267
8.43	957	8.25	1789	8.40	3295
8.53	986	8.35	1817	8.51	3291
8.63	955	8.46	1815	8.61	3287
8.72	954	8.56	1783	8.72	3314
8.84	983	8.66	1781	8.82	3311
8.94	952	8.76	1809	8.92	3338
9.04	951	8.86	1838	9.02	3334
9.14	950	8.96	1836	9.13	3361
9.24	949	9.06	1833	9.23	3357
9.36	947	9.16	1831	9.33	3323
9.46	946	9.26	1799	9.44	3349
9.55	915	9.36	1827	9.54	3376
9.67	884	9.46	1825	9.64	3373

9.75	883	9.56	1823	9.74	3369
9.87	912	9.66	1821	9.84	3365
9.97	881	9.76	1819	9.95	3361
10.07	880	9.87	1787	10.05	3387
10.17	909	9.97	1786	10.15	3384
10.27	908	10.06	1843	10.25	3410
10.39	907	10.16	1841	10.36	3406
10.48	876	10.27	1809	10.46	3402
10.58	935	10.37	1866	10.57	3398
10.68	934	10.47	1864	10.67	3395
10.78	933	10.57	1862	10.77	3421
10.90	931	10.67	1801	10.87	3417
11.00	930	10.77	1828	10.97	3443
11.10	959	10.87	1856	11.08	3469
11.20	928	10.97	1942	11.18	3435
11.30	927	11.07	1852	11.28	3491
11.39	926	11.17	1879	11.38	3457
11.51	954	11.28	1877	11.48	3483
11.61	953	11.37	1816	11.59	3449
11.71	952	11.47	1931	11.69	3475
11.81	980	11.58	1812	11.79	3501
11.91	979	11.68	1926	11.89	3527
12.03	978	11.78	1808	12.00	3522
12.13	977	11.88	1864	12.10	3489
12.23	1005	11.98	1833	12.20	3544
12.32	975	12.08	1860	12.30	3540
12.42	1003	12.18	1886	12.41	3506
12.54	1001	12.28	1884	12.51	3561
12.64	1000	12.38	1911	12.61	3557
12.74	1028	12.48	1909	12.72	3553
12.84	1027	12.58	1907	12.82	3549
12.94	1025	12.68	1904	12.92	3515
13.06	995	12.78	1902	13.02	3540
13.16	1023	12.88	1900	13.13	3536
13.25	1022	12.99	1898	13.23	3532
13.35	992	13.08	1896	13.33	3528

13.45	991	13.19	1893	13.43	3553
13.57	989	13.29	1891	13.54	3548
13.67	988	13.39	1918	13.64	3515
13.77	987	13.49	1887	13.74	3540
13.87	957	13.59	1885	13.84	3536
13.97	985	13.69	1996	13.95	3532
14.09	955	13.79	1909	14.05	3557
14.18	982	13.89	1935	14.15	3552
14.28	981	13.99	1876	14.26	3577
14.38	1008	14.09	1902	14.36	3573
14.48	1007	14.19	1900	14.46	3569
14.60	1034	14.29	1926	14.56	3593
14.70	1033	14.39	1924	14.66	3560
14.80	1032	14.50	1921	14.77	3556
14.90	1031	14.59	1947	14.87	3580
15.00	1058	14.69	1917	14.97	3576
15.11	1084	14.80	1914	15.07	3600
15.21	1083	14.90	1912	15.18	3625
15.31	1082	15.00	1938	15.28	3592
15.41	1081	15.10	1964	15.38	3644
15.51	1107	15.20	1905	15.49	3640
15.63	1106	15.30	1959	15.59	3635
15.73	1132	15.40	1985	15.69	3660
15.83	1131	15.50	1982	15.79	3655
15.92	1158	15.60	1952	15.90	3651
16.02	1156	15.71	1950	16.00	3675
16.14	1155	15.80	1975	16.10	3670
16.24	1153	15.91	1945	16.20	3666
16.34	1180	16.00	1915	16.30	3690
16.44	1178	16.11	1940	16.41	3713
16.54	1177	16.21	1966	16.51	3709
16.64	1203	16.31	1963	16.61	3760
16.76	1201	16.41	1961	16.71	3756
16.85	1200	16.50	1986	16.82	3751
16.95	1198	16.61	2011	16.92	3747
17.05	1197	16.71	1954	17.03	3742

17.15	1196	16.81	1979	17.12	3737
17.27	1194	16.91	1949	17.23	3761
17.37	1192	17.01	1974	17.33	3756
17.47	1191	17.11	1972	17.43	3779
17.57	1190	17.21	1969	17.54	3747
17.67	1188	17.31	1967	17.64	3770
17.78	1186	17.41	2019	17.74	3738
17.88	1185	17.51	2017	17.84	3761
17.98	1184	17.62	2014	17.95	3728
18.08	1182	17.72	2012	18.05	3723
18.18	1181	17.81	1982	18.15	3746
18.30	1179	17.91	2007	18.25	3742
18.40	1205	18.02	2004	18.36	3709
18.50	1203	18.12	2029	18.46	3705
18.60	1202	18.22	1999	18.56	3700
18.69	1200	18.32	1997	18.66	3723
18.81	1225	18.42	1994	18.77	3746
18.91	1197	18.52	1992	18.87	3713
19.01	1222	18.62	2016	18.97	3764
19.11	1248	18.72	1987	19.07	3732
19.21	1246	18.82	2011	19.17	3754
19.33	1244	18.92	2009	19.28	3777
19.43	1270	19.03	2033	19.38	3799
19.53	1268	19.12	2004	19.48	3767
19.62	1293	19.22	2001	19.59	3790
19.72	1292	19.33	1999	19.69	3785
		19.43	1996	19.79	3807
		19.53	2047	19.89	3802
		19.62	1991	20.00	3797
		19.73	2042	20.10	3792
		19.83	2039		
		19.93	1984		
		20.03	2034		

Rf	0.98		**Ei**	**B**	**σ3**	**Ei**	**B**	**σ3**	**Ei**	**B**	**σ3**

Rf	0.98
c	0.00
Pa	2116	psf
K	1000
n	0.45

Ei	**B**	**σ3**	**Ei**	**B**	**σ3**	**Ei**	**B**	**σ3**
862502.25	0.00	288.00	1370516.86	0.00	806.00	1950153.22	0.00	1765.00

1/(σ1-σ3)ult

1.06E-03
5.65E-04
2.71E-04

Axial Strain	Deviator Stress	Hyperbolic σ1-σ3	Axial Strain	Deviator Stress	Hyperbolic σ1-σ3	Axial Strain	Deviator Stress	Hyperbolic σ1-σ3
0.00	83.63	0.0	0.00	136.76	0	0.00	47.95	0
0.10	613.57	447.2	0.10	960.06	783.2	0.10	1162.20	1285.4
0.20	811.52	606.1	0.20	1255.24	1081.9	0.20	1397.13	1916.4
0.30	876.83	687.5	0.30	1352.62	1239.4	0.31	1159.80	2285.4
0.42	941.83	744.7	0.40	1416.90	1341.6	0.41	1158.58	2531.5
0.51	973.89	775.7	0.50	1481.08	1409.7	0.51	1123.80	2695.8
0.61	972.92	798.2	0.60	1545.13	1459.1	0.62	1660.09	2826.0
0.71	1037.79	815.3	0.71	1543.57	1496.6	0.72	1826.19	2922.8
0.81	1036.76	828.7	0.81	1542.01	1526.1	0.82	1891.38	3000.1
0.91	1035.73	839.5	0.91	1540.42	1550.3	0.92	1956.36	3065.6
1.03	1001.67	850.0	1.01	1571.50	1569.8	1.03	2054.72	3118.0
1.13	1033.45	857.2	1.11	1635.11	1586.1	1.13	2119.38	3163.9
1.23	1032.42	863.4	1.21	1633.48	1599.7	1.23	2150.55	3202.3
1.33	998.66	868.7	1.31	1696.90	1611.7	1.33	2215.05	3234.9
1.42	997.66	873.3	1.41	1695.14	1622.3	1.44	2212.78	3263.5
1.54	996.46	878.1	1.51	1628.50	1631.2	1.53	2277.12	3288.2
1.64	995.46	881.6	1.61	1691.69	1639.4	1.64	2307.94	3311.6
1.74	961.88	884.7	1.71	1689.96	1646.6	1.74	2371.94	3332.0
1.84	993.46	887.5	1.81	1655.86	1653.0	1.85	2402.63	3350.3
1.94	992.46	890.0	1.91	1718.85	1658.8	1.95	2433.30	3366.6
2.06	958.78	892.8	2.01	1684.75	1664.2	2.05	2463.85	3381.7
2.16	957.81	894.9	2.12	1683.02	1669.0	2.15	2527.50	3394.9

2.26	989.25	896.7	2.21	1681.36	1673.2	2.26	2491.64	3408.3
2.35	955.88	898.5	2.31	1647.39	1677.3	2.36	2522.12	3419.4
2.45	954.91	900.1	2.41	1677.87	1680.9	2.46	2552.43	3430.1
2.57	986.05	901.9	2.52	1676.15	1684.4	2.56	2582.67	3440.0
2.67	1017.32	903.2	2.62	1674.38	1687.6	2.67	2645.68	3449.3
2.77	984.05	904.5	2.72	1672.66	1690.5	2.77	2642.98	3457.5
2.87	**983.05**	905.7	2.82	1670.90	1693.3	**2.87**	**2673.01**	3465.5
2.97	982.05	906.8	2.92	1669.17	1695.9	2.97	2670.28	3472.7
3.09	980.85	908.0	3.02	1667.44	1698.3	3.08	2700.15	3479.8
3.18	1011.95	909.0	3.12	1665.78	1700.4	3.18	2762.73	3486.3
3.28	1010.91	909.9	3.22	1664.02	1702.6	3.28	2759.73	3492.6
3.38	1009.88	910.7	3.32	1630.39	1704.6	3.38	2789.56	3498.2
3.48	1008.85	911.5	3.42	1660.57	1706.4	3.49	2786.59	3503.7
3.60	1007.61	912.5	3.52	1690.65	1708.2	3.59	2783.55	3509.0
3.70	1006.57	913.2	3.62	1720.63	1709.9	3.69	2845.74	3513.8
3.80	1005.54	913.9	3.72	1718.88	1711.5	3.79	2842.75	3518.4
3.90	1004.50	914.5	3.82	1653.63	1713.0	3.90	2839.70	3522.9
4.00	1003.47	915.1	3.93	1683.54	1714.5	4.00	2869.11	3527.1
4.11	970.43	915.8	4.03	1713.42	1715.9	4.10	2898.50	3531.0
4.21	969.43	916.4	4.13	1711.63	1717.2	4.20	2863.00	3534.8
4.31	968.43	916.9	4.23	1709.84	1718.4	4.31	2892.27	3538.5
4.41	999.13	917.4	4.33	1676.47	1719.6	4.41	2889.15	3542.0
4.51	966.43	917.9	4.43	1737.76	1720.7	4.51	2918.37	3545.3
4.63	996.85	918.5	4.53	1735.94	1721.8	4.61	2915.28	3548.4
4.73	964.23	918.9	4.63	1702.70	1722.8	4.72	2944.28	3551.5
4.83	963.23	919.3	4.73	1763.70	1723.8	4.82	2973.20	3554.5
4.93	962.23	919.7	4.83	1699.11	1724.8	4.92	3002.24	3557.2
5.0	961.2	920.1	4.93	1759.94	1725.71	5.02	2998.99	3559.9
5.1	928.6	920.6	5.03	1726.80	1726.57	5.13	3027.73	3562.6
5.2	927.6	920.9	5.13	1724.94	1727.43	5.23	3024.57	3565.0
5.3	926.6	921.3	5.23	1691.91	1728.23	5.34	3053.08	3567.5
5.4	925.7	921.6	5.34	1721.29	1729.03	5.43	3049.95	3569.7
5.5	924.7	921.9	5.44	1781.82	1729.78	5.54	3046.56	3572.0
5.7	923.5	922.3	5.53	1686.53	1730.50	5.64	3075.3	3574.07
5.8	922.6	922.6	5.64	1746.92	1731.22	5.74	3071.9	3576.16

5.9	921.6	922.9	5.74	1713.95	1731.91	5.85	3068.5	3578.17
6.0	920.6	923.2	5.84	1712.16	1732.55	5.95	3097.0	3580.09
6.1	919.7	923.5	5.94	1710.33	1733.19	6.05	3093.6	3581.97
6.2	918.7	923.7	6.04	1708.51	1733.80	6.15	3090.2	3583.83
6.3	917.5	924.0	6.14	1706.68	1734.40	6.26	3118.5	3585.56
6.4	916.6	924.3	6.24	1735.77	1734.97	6.36	3083.5	3587.24
6.5	915.6	924.5	6.34	1764.75	1735.54	6.46	3080.1	3588.89
6.6	914.6	924.7	6.44	1762.86	1736.08	6.56	3076.7	3590.50
6.7	913.7	925.0	6.54	1730.15	1736.61	6.67	3104.8	3592.09
6.8	912.5	925.2	6.64	1728.29	1737.11	6.77	3101.5	3593.54
6.9	911.5	925.4	6.74	1757.18	1737.61	6.87	3098.1	3595.01
7.0	910.6	925.6	6.84	1755.33	1738.08	6.98	3126.0	3596.47
7.1	909.6	925.8	6.95	1753.36	1738.56	7.07	3154.2	3597.77
7.2	908.6	926.0	7.05	1751.43	1739.02	7.18	3150.6	3599.15
7.3	938.2	926.3	7.15	1749.61	1739.45	7.28	3209.8	3600.46
7.4	967.9	926.4	7.25	1747.68	1739.88	7.38	3206.2	3601.73
7.5	966.9	926.6	7.35	1745.79	1740.30	7.48	3202.7	3602.95
7.6	965.8	926.8	7.45	1743.89	1740.71	7.59	3199.1	3604.18
7.7	964.8	927.0	7.55	1742.00	1741.10	7.69	3226.7	3605.36
7.8	963.6	927.2	7.65	1770.52	1741.49	7.79	3254.4	3606.46
7.9	962.5	927.3	7.75	1768.63	1741.86	7.90	3250.8	3607.58
8.0	992.0	927.5	7.85	1827.51	1742.22	8.00	3278.2	3608.67
8.1	960.5	927.6	7.95	1795.09	1742.59	8.10	3274.6	3609.73
8.2	989.9	927.8	8.05	1793.17	1742.93	8.21	3270.8	3610.79
8.3	958.2	927.9	8.15	1760.93	1743.27	8.31	3267.3	3611.76
8.4	957.2	928.1	8.25	1789.22	1743.61	8.40	3294.7	3612.71
8.5	986.5	928.2	8.35	1817.47	1743.93	8.51	3290.9	3613.70
8.6	955.1	928.4	8.46	1815.48	1744.25	8.61	3287.2	3614.64
8.7	954.1	928.5	8.56	1783.34	1744.55	8.72	3314.3	3615.58
8.8	983.0	928.6	8.66	1781.34	1744.86	8.82	3310.6	3616.48
8.9	951.8	928.8	8.76	1809.47	1745.16	8.92	3337.6	3617.35
9.0	950.7	928.9	8.86	1837.52	1745.44	9.02	3334.0	3618.18
9.1	949.7	929.0	8.96	1835.58	1745.71	9.13	3360.8	3619.04
9.2	948.7	929.1	9.06	1833.47	1746.00	9.23	3357.1	3619.84
9.4	947.4	929.3	9.16	1831.49	1746.26	9.33	3322.7	3620.63

9.5	946.4	929.4	9.26	1799.47	1746.54	9.44	3349.5	3621.43
9.6	915.4	929.5	9.36	1827.44	1746.79	9.54	3376.2	3622.20
9.7	884.2	929.6	9.46	1825.33	1747.05	9.64	3372.5	3622.93
9.8	883.4	929.7	9.56	1823.39	1747.29	9.74	3368.7	3623.67
9.9	912.2	929.8	9.66	1821.32	1747.53	9.84	3364.8	3624.39
10.0	881.3	929.9	9.76	1819.30	1747.77	9.95	3361.0	3625.10
10.1	880.4	930.0	9.87	1787.48	1748.01	10.05	3387.5	3625.81
10.2	909.2	930.1	9.97	1785.52	1748.24	10.15	3383.7	3626.48
10.3	908.2	930.2	10.06	1842.88	1748.45	10.25	3410.2	3627.13
10.4	907.0	930.3	10.16	1840.82	1748.67	10.36	3406.2	3627.80
10.5	876.3	930.4	10.27	1809.17	1748.89	10.46	3402.4	3628.42
10.6	934.6	930.5	10.37	1866.21	1749.10	10.57	3398.3	3629.09
10.7	933.6	930.6	10.47	1864.17	1749.31	10.67	3394.6	3629.67
10.8	932.5	930.7	10.57	1862.03	1749.51	10.77	3420.8	3630.29
10.9	931.3	930.8	10.67	1801.07	1749.71	10.87	3417.0	3630.86
11.0	930.3	930.9	10.77	1828.43	1749.91	10.97	3443.1	3631.44
11.1	958.7	930.9	10.87	1855.76	1750.10	11.08	3469.1	3632.03
11.2	928.2	931.0	10.97	1941.73	1750.29	11.18	3435.0	3632.59
11.3	927.2	931.1	11.07	1851.58	1750.47	11.28	3491.2	3633.12
11.4	926.1	931.2	11.17	1878.73	1750.66	11.38	3457.2	3633.67
11.5	954.2	931.3	11.28	1876.56	1750.84	11.48	3483.2	3634.19
11.6	953.2	931.3	11.37	1816.04	1751.01	11.59	3449.1	3634.74
11.7	952.1	931.4	11.47	1930.73	1751.18	11.69	3475.0	3635.23
11.8	980.3	931.5	11.58	1811.88	1751.35	11.79	3500.8	3635.74
11.9	979.2	931.6	11.68	1926.31	1751.52	11.89	3526.6	3636.23
12.0	977.9	931.6	11.78	1807.77	1751.68	12.00	3522.4	3636.73
12.1	976.8	931.7	11.88	1863.82	1751.85	12.10	3488.6	3637.20
12.2	1004.8	931.8	11.98	1832.71	1752.00	12.20	3543.9	3637.66
12.3	974.6	931.8	12.08	1859.57	1752.16	12.30	3539.8	3638.13
12.4	1002.5	931.9	12.18	1886.44	1752.31	12.41	3506.0	3638.59
12.5	1001.1	932.0	12.28	1884.24	1752.46	12.51	3560.9	3639.05
12.6	1000.0	932.0	12.38	1911.02	1752.61	12.61	3556.9	3639.47
12.7	1027.8	932.1	12.48	1908.78	1752.76	12.72	3552.7	3639.91
12.8	1026.6	932.2	12.58	1906.55	1752.90	12.82	3548.5	3640.34
12.9	1025.5	932.2	12.68	1904.36	1753.04	12.92	3514.9	3640.76

13.1	995.3	932.3	12.78	1902.21	1753.18	13.02	3540.2	3641.17
13.2	1022.9	932.4	12.88	1900.02	1753.32	13.13	3535.9	3641.59
13.3	1021.8	932.4	12.99	1897.79	1753.45	13.23	3531.8	3641.98
13.4	991.9	932.5	13.08	1895.64	1753.58	13.33	3527.7	3642.37
13.5	990.7	932.5	13.19	1893.41	1753.72	13.43	3552.8	3642.77
13.6	989.4	932.6	13.29	1891.21	1753.85	13.54	3548.4	3643.16
13.7	988.2	932.6	13.39	1917.58	1753.97	13.64	3515.1	3643.53
13.8	987.1	932.7	13.49	1886.79	1754.10	13.74	3540.1	3643.90
13.9	957.4	932.8	13.59	1884.69	1754.22	13.84	3535.9	3644.27
14.0	984.8	932.8	13.69	1996.24	1754.34	13.95	3531.7	3644.63
14.1	955.0	932.9	13.79	1908.60	1754.47	14.05	3556.6	3644.98
14.2	982.3	932.9	13.89	1934.81	1754.58	14.15	3552.2	3645.35
14.3	981.2	933.0	13.99	1875.88	1754.69	14.26	3577.0	3645.69
14.4	1008.5	933.0	14.09	1902.02	1754.81	14.36	3572.7	3646.03

Comparison Hyperbolic vs. Test Data (Deviator Stress vs. Axial Strain)-Fill
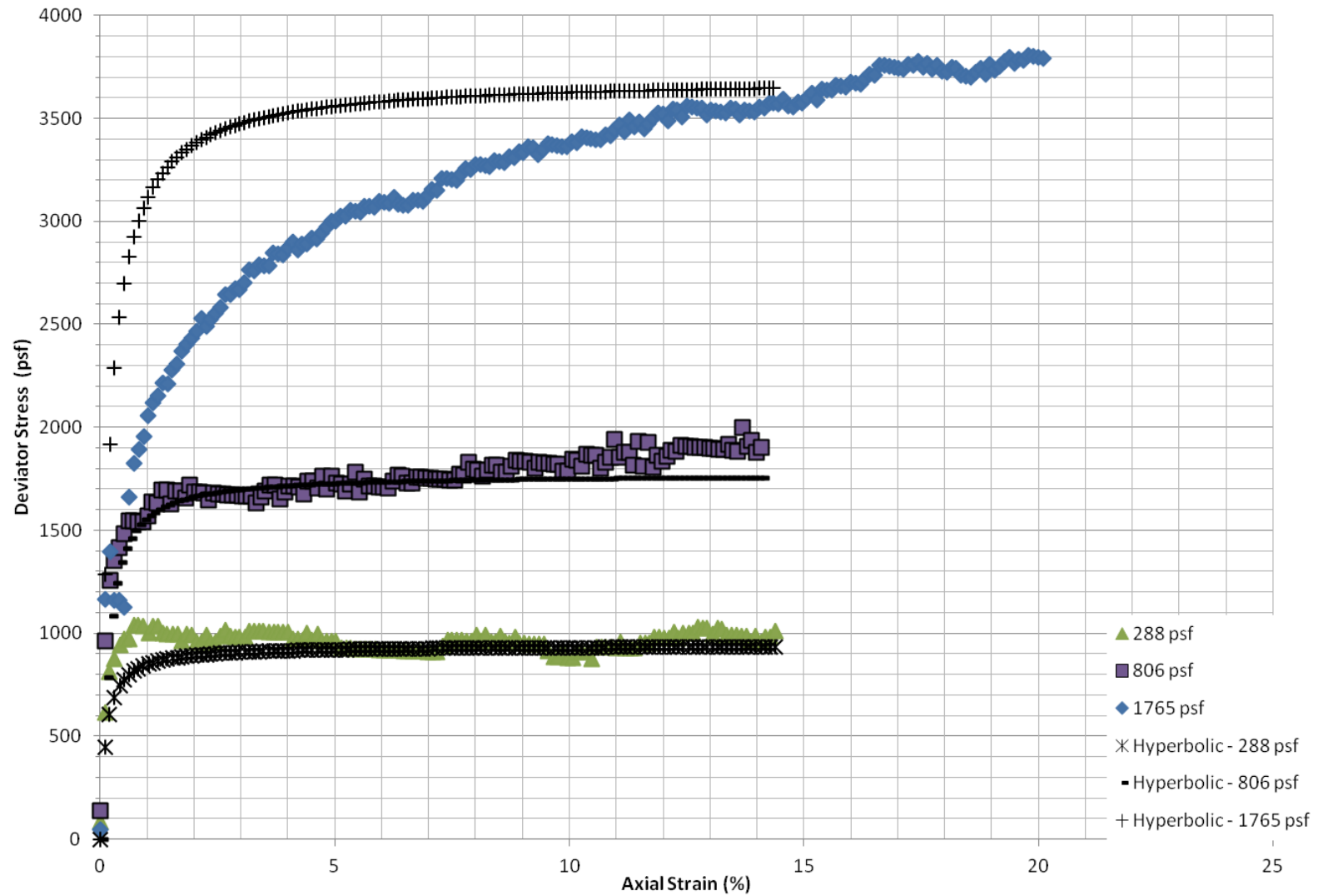
Soil: Dessicated Crust   2F-01-29

Confining Pressures		Data for Deviatoric Modulus Parameters						
		70% Stress Level				95% Stress Level		
σ_3	$(\sigma_1-\sigma_3)_f$	$\sigma_1-\sigma_3$	ε_a	$\varepsilon_a/(\sigma_1-\sigma_3)$		$\sigma_1-\sigma_3$	ε_a	$\varepsilon_a/(\sigma_1-\sigma_3)$
246	1134	793.8	0.032	4.03E-05		1077.3	0.047	4.36E-05
910	2628	1839.6	0.015	8.15E-06		2496.6	0.041	1.64E-05
1588	3910	2737	0.006	2.19E-06		3714.5	0.025	6.73E-06

$P_a=$ 2116   psf

σ_3/P_a	$1/(\sigma_1-\sigma_3)_{ult}$	R_f	E_i/P_a
0.1	2.21E-04	0.25	14
0.4	3.18E-04	0.84	140
0.8	2.39E-04	0.93	623

R_f Average=   0.67

Raw Test Data
Confining
Pressures
Sigma 3

psf	Pa (psf)	Sigma3/Pa
246	2116	0.116257089
910	2116	0.430056711
1588	2116	0.75047259

Sigma 3 = 9390 psf	Axial Strain	Deviator Stress	Sigma 3 =10140 psf	Axial Strain	Deviator Stress	Sigma 3 = 11640 psf	Axial Strain	Deviator Stress
	0.0	0		0.0	0		0.0	0
	0.1	164		0.1	190		0.1	603
	0.2	220		0.2	497		0.2	1152
	0.3	254		0.3	836		0.3	1710
	0.4	237		0.4	1001		0.4	2193
	0.5	270		0.5	1165		0.5	2517
	0.6	298		0.6	1258		0.6	2746
	0.7	326		0.7	1343		0.7	2901
	0.8	342		0.8	1413		0.8	3035
	0.9	353		0.9	1482		0.9	3168
	1.0	375		1.0	1551		1.0	3238
	1.3	408		1.3	1695		1.3	3428
	1.5	457		1.5	1831		1.5	3534
	1.8	500		1.8	1958		1.8	3598
	2.0	549		2.0	2077		2.0	3630
	2.3	597		2.3	2141		2.3	3673
	2.5	646		2.6	2205		2.5	3715
	2.8	699		2.8	2276		2.8	3756
	3.0	757		3.1	2324		3.0	3777
	3.3	810		3.3	2371		3.3	3798
	3.5	857		3.6	2426		3.5	3809
	3.8	899		3.8	2458		3.8	3850
	4.0	956		4.1	2497		4.1	3850
	4.5	1054		4.6	2567		4.6	3880

5.1	1134	5.1	2628	5.1	3910
5.6	1230	5.6	2681	5.6	3909
6.1	1324	6.1	2711	6.1	3927
6.6	1386	6.6	2733	6.6	3946
7.1	1447	7.1	2777	7.1	3964
7.6	1507	7.7	2791	7.6	3981
8.1	1556	8.2	2827	8.1	3979
8.6	1594	8.7	2840	8.6	3976
9.1	1636	9.2	2867	9.1	3974
9.6	1673	9.7	2872	9.6	3970
10.1	1694	10.2	2877	10.1	3977
10.6	1725	10.7	2875	10.6	3964
11.1	1761	11.2	2873	11.1	3941
11.6	1791	11.7	2870	11.7	3919
12.1	1806	12.2	2861	12.2	3896
13.1	1795	12.8	2851	12.7	3874
13.6	1799	13.3	2827	13.2	3842
14.1	1803	13.8	2818	13.7	3792
14.6	1807	14.3	2801	14.2	3761
15.2	1825	14.8	2784	14.7	3730
				15.2	3699

Rf	0.67	
c	0.00	
Pa	2116	psf
K	1400	
n	2.7	

1/(σ1-σ3)ult

2.21E-04
3.18E-04
2.39E-04

Ei	B	σ3	Ei	B	σ3	Ei	B	σ3
8877.20	0.00	246.00	303503.13	0.00	910.00	1364733.19	0.00	1588.00

Axial Strain	Deviator Stress	Hyperbolic σ1-σ3	Axial Strain	Deviator Stress	Hyperbolic σ1-σ3	Axial Strain	Deviator Stress	Hyperbolic σ1-σ3
0.0	0	0.0	0.0	0	0	0.0	0	0
0.1	164	8.9	0.1	190	276.8	0.1	603	1029.2
0.2	220	17.7	0.2	497	508.8	0.2	1152	1652.3
0.3	254	26.5	0.3	836	706.1	0.3	1710	2070.0
0.4	237	35.2	0.4	1001	875.9	0.4	2193	2369.5
0.5	270	44.0	0.5	1165	1023.6	0.5	2517	2594.7
0.6	298	52.6	0.6	1258	1153.2	0.6	2746	2770.3
0.7	326	61.3	0.7	1343	1267.9	0.7	2901	2911.0
0.8	342	69.9	0.8	1413	1370.1	0.8	3035	3026.2
0.9	353	78.5	0.9	1482	1461.8	0.9	3168	3122.4
1.0	375	87.1	1.0	1551	1544.4	1.0	3238	3203.8
1.3	408	112.5	1.3	1695	1749.9	1.3	3428	3387.3
1.5	457	129.4	1.5	1831	1859.9	1.5	3534	3475.8
1.8	500	154.3	1.8	1958	1995.8	1.8	3598	3577.0
2.0	549	170.8	2.0	2077	2071.4	2.0	3630	3629.9
2.3	597	195.4	2.3	2141	2167.9	2.3	3673	3694.0
2.5	646	211.6	2.6	2205	2248.5	2.5	3715	3729.1
2.8	699	235.6	2.8	2276	2295.2	2.8	3756	3773.3
3.0	757	251.5	3.1	2324	2356.8	3.0	3777	3798.3
3.3	810	275.1	3.3	2371	2393.2	3.3	3798	3830.6
3.5	857	290.7	3.6	2426	2441.8	3.5	3809	3849.3
3.8	899	313.9	3.8	2458	2470.8	3.8	3850	3873.9

4.0	956	329.2	4.1	2497	2510.2	4.1	3850	3895.2
4.5	1054	367.1	4.6	2567	2566.5	4.6	3880	3924.9
5.1	1134	411.6	5.1	2628	2613.6	5.1	3910	3949.1
5.6	1230	447.9	5.6	2681	2653.6	5.6	3909	3969.2
6.1	1324	483.6	6.1	2711	2688.0	6.1	3927	3986.2
6.6	1386	518.7	6.6	2733	2717.9	6.6	3946	4000.7
7.1	**1447**	553.2	**7.1**	**2777**	2744.1	**7.1**	**3964**	4013.3
7.6	1507	587.1	7.7	2791	2771.6	7.6	3981	4024.2
8.1	1556	620.5	8.2	2827	2791.8	8.1	3979	4033.9
8.6	1594	653.2	8.7	2840	2809.9	8.6	3976	4042.5
9.1	1636	685.4	9.2	2867	2826.2	9.1	3974	4050.1
9.6	1673	717.1	9.7	2872	2841.1	9.6	3970	4057.0
10.1	1694	748.3	10.2	2877	2854.6	10.1	3977	4063.3
10.6	1725	779.0	10.7	2875	2866.9	10.6	3964	4068.9
11.1	1761	809.2	11.2	2873	2878.3	11.1	3941	4074.1
11.6	1791	838.8	11.7	2870	2888.7	11.7	3919	4079.7
12.1	1806	868.1	12.2	2861	2898.4	12.2	3896	4084.0
13.1	1795	925.1	12.8	2851	2909.0	12.7	3874	4087.9
13.6	1799	953.0	13.3	2827	2917.3	13.2	3842	4091.6
14.1	1803	980.5	13.8	2818	2924.9	13.7	3792	4095.0
14.6	1807	1007.5	14.3	2801	2932.1	14.2	3761	4098.1
15.2	1825	1039.4	14.8	2784	2938.8	14.70	3730.00	4101.1
						15.20	3699.00	4103.9

Comparison Hyperbolic vs. Test Data (Deviator Stress vs. Axial Strain) - Dessicated Clay
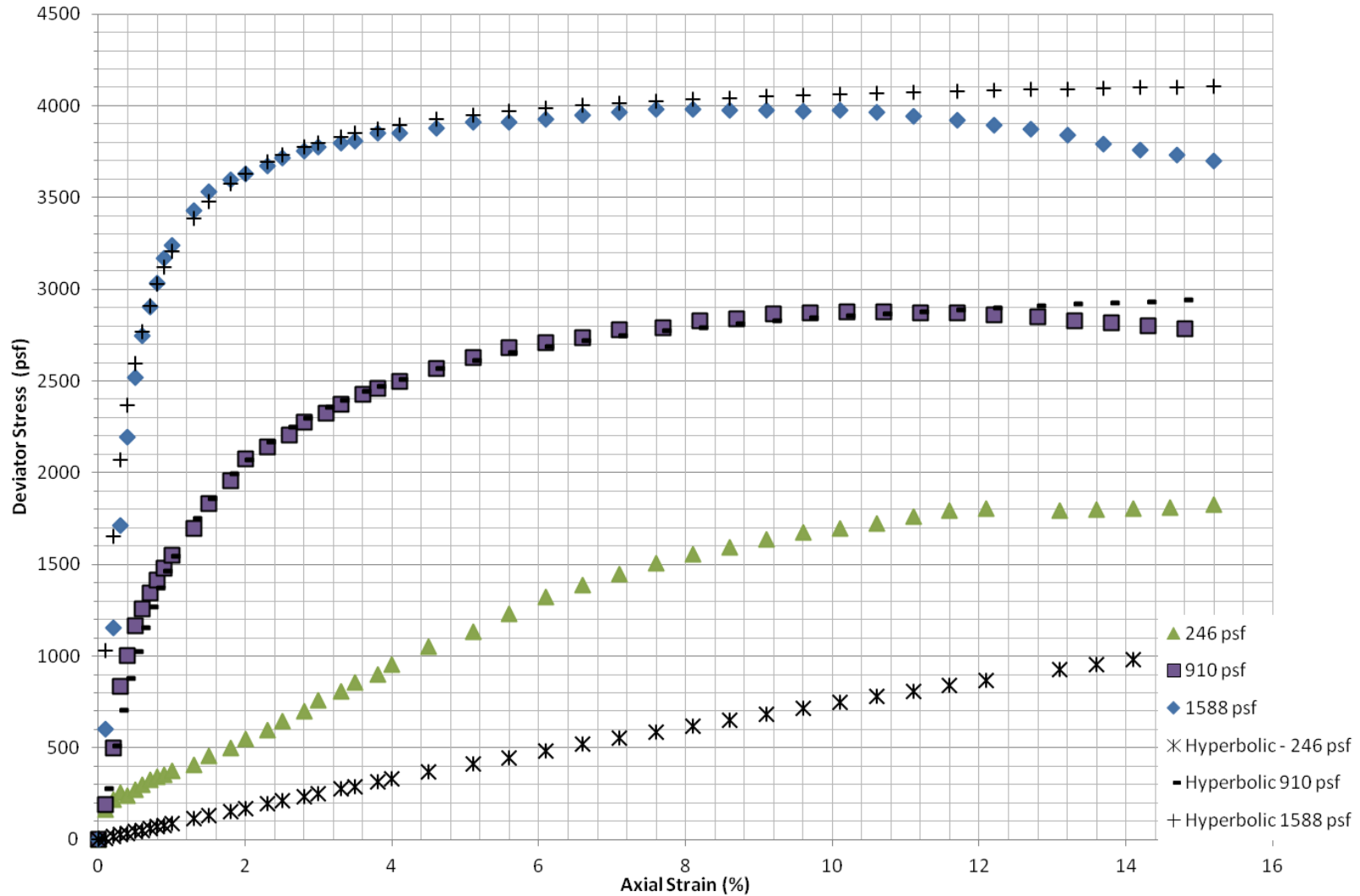
Soil: Upper Soft Soil   SRE-09-04

Confining Pressures		Data for Deviatoric Modulus Parameters						
		70% Stress Level				95% Stress Level		
σ_3	$(\sigma_1-\sigma_3)_f$	$\sigma_1-\sigma_3$	ε_a	$\varepsilon_a/(\sigma_1-\sigma_3)$	$\sigma_1-\sigma_3$	ε_a	$\varepsilon_a/(\sigma_1-\sigma_3)$
173	566	396.2	0.0015	3.79E-06	537.7	0.0066	1.23E-05
389	926	648.2	0.0033	5.09E-06	879.7	0.0133	1.51E-05
878	1864	1304.8	0.0045	3.45E-06	1770.8	0.0158	8.92E-06

P_a=   2116   psf

σ_3/P_a	$1/(\sigma_1-\sigma_3)_{ult}$	R_f	E_i/P_a
0.1	1.66E-03	0.94	367
0.2	1.00E-03	0.93	265
0.4	4.84E-04	0.90	372

R_f Average=   0.92

Raw Test Data
Confining
Pressures
Sigma 3

psf	Pa (psf)	Sigma3/Pa
173	2116	0.081758034
389	2116	0.183837429
878	2116	0.414933837

Sigma 3 = 346 psf	Axial Strain	Deviator Stress	Sigma 3 =389 psf	Axial Strain	Deviator Stress	Sigma 3 = 878 psf	Axial Strain	Deviator Stress
	0.00	129		0.00	58		0.00	36
	0.08	362		0.08	172		0.10	664
	0.18	409		0.16	470		0.20	1007
	0.26	455		0.25	538		0.30	1208
	0.35	478		0.33	629		0.40	1388
	0.43	501		0.41	697		0.50	1467
	0.51	523		0.49	742		0.59	1526
	0.61	523		0.58	787		0.69	1605
	0.69	546		0.66	809		0.79	1624
	0.77	568		0.74	808		0.89	1682
	0.86	545		0.82	830		0.99	1701
	0.94	567		0.91	852		1.09	1699
	1.04	567		0.99	852		1.19	1717
	1.12	589		1.07	851		1.29	1756
	1.20	589		1.15	873		1.39	1754
	1.28	588		1.24	872		1.49	1752
	1.37	588		1.32	894		1.58	1770
	1.45	587		1.40	893		1.68	1748
	1.55	587		1.48	893		1.78	1767
	1.63	586		1.57	892		1.88	1745
	1.71	586		1.65	891		1.98	1763
	1.79	608		1.73	890		2.08	1781
	1.88	585		1.81	912		2.18	1799
	1.97	607		1.90	889		2.28	1797

2.06	607	1.98	888	2.38	1776
2.14	583	2.06	887	2.48	1734
2.22	583	2.14	887	2.57	1772
2.30	582	2.23	886	2.67	1770
2.40	559	2.31	885	2.77	1828
2.48	559	2.39	884	2.87	1806
2.57	535	2.47	884	2.97	1804
2.65	535	2.55	883	3.07	1802
2.73	534	2.64	904	3.17	1781
2.83	534	2.72	904	3.27	1779
2.91	511	2.80	903	3.37	1797
2.99	510	2.88	880	3.47	1815
3.08	533	2.97	946	3.56	1813
3.16	532	3.05	901	3.66	1811
3.26	532	3.13	878	3.76	1809
3.34	554	3.21	899	3.86	1827
3.42	531	3.30	920	3.96	1805
3.50	553	3.38	898	4.06	1823
3.59	552	3.46	941	4.16	1821
3.68	574	3.54	896	4.26	1819
3.77	574	3.64	895	4.36	1837
3.85	573	3.71	917	4.46	1815
3.93	573	3.79	894	4.55	1833
4.01	572	3.87	937	4.65	1831
4.11	572	3.97	892	4.75	1868
4.19	571	4.05	891	4.85	1846
4.28	571	4.14	890	4.95	1864
4.36	592	4.20	934	5.05	1881
4.44	614	4.30	911	5.15	1841
4.54	614	4.37	910	5.25	1877
4.62	591	4.45	888	5.35	1837
4.70	613	4.55	909	5.45	1873
4.79	590	4.63	908	5.54	1852
4.87	567	4.71	907	5.64	1869
4.97	566	4.78	885	5.74	1867
5.05	544	4.88	905	5.84	1846

5.13	565	4.96	926	5.94	1863
5.21	565	5.03	904	6.04	1842
5.30	565	5.13	925	6.14	1821
5.39	564	5.21	902	6.24	1838
5.48	563	5.29	923	6.34	1855
5.56	563	5.37	901	6.44	1853
5.64	562	5.46	922	6.53	1852
5.72	562	5.54	942	6.63	1812
5.81	539	5.62	898	6.73	1848
5.90	539	5.70	941	6.83	1846
5.99	538	5.79	918	6.93	1844
6.07	538	5.87	874	7.03	1861
6.15	516	5.95	938	7.13	1859
6.23	515	6.03	894	7.23	1857
6.33	515	6.12	915	7.33	1855
6.41	536	6.20	893	7.43	1871
6.50	536	6.28	914	7.52	1888
6.58	535	6.36	913	7.62	1905
6.66	535	6.44	955	7.72	1884
6.76	534	6.53	954	7.82	1863
6.84	555	6.61	953	7.92	1880
6.94	533	6.69	952	8.02	1878
7.01	554	6.77	951	8.12	1895
7.09	576	6.86	929	8.22	1893
7.19	553	6.94	950	8.32	1891
7.27	509	7.02	949	8.42	1888
7.35	509	7.10	948	8.51	1886
7.43	530	7.19	947	8.61	1884
7.52	551	7.27	946	8.71	1882
7.62	551	7.35	924	8.81	1899
7.70	550	7.43	945	8.91	1915
7.78	571	7.52	944	9.01	1876
7.86	571	7.60	943	9.11	1874
7.94	570	7.68	942	9.23	1890
8.04	548	7.76	941	9.31	1870
8.13	569	7.85	941	9.41	1886

8.21	547	7.93	940	9.52	1902
8.29	547	8.01	939	9.62	1918
8.37	525	8.09	938	9.70	1880
8.47	546	8.18	958	9.80	1878
8.55	545	8.26	936	9.92	1912
8.63	545	8.34	935	10.02	1892
8.72	544	8.42	935	10.12	1926
8.80	544	8.51	934	10.22	1924
8.90	522	8.59	933	10.32	1904
8.98	521	8.67	932	10.42	1902
9.06	521	8.75	931	10.51	1881
9.14	520	8.83	930	10.61	1934
9.23	520	8.92	909	10.71	1895
9.33	519	9.00	950	10.81	1929
9.41	519	9.08	949	10.91	1927
9.49	518	9.16	927	11.01	1889
9.57	518	9.25	947	11.11	1905
9.65	517	9.33	925	11.21	1903
9.75	517	9.41	925	11.31	1883
9.84	537	9.49	944	11.41	1899
9.92	537	9.58	944	11.50	1914
10.00	536	9.66	963	11.60	1912
10.08	557	9.74	963	11.70	1928
10.16	556	9.82	941	11.80	1908
10.26	556	9.91	940	11.90	1906
10.35	555	9.99	960	12.00	1922
10.43	555	10.07	959	12.10	1919
10.51	575	10.15	958	12.20	1899
10.59	554	10.24	978	12.30	1915
10.69	574	10.32	977	12.40	1913
10.77	574	10.40	935	12.50	1928
10.86	573	10.48	955	12.59	1891
10.94	572	10.57	974	12.69	1924
11.02	572	10.65	953	12.79	1940
11.12	571	10.73	932	12.89	1920
11.20	591	10.81	972	12.99	1935

11.28	570	10.90	950	13.09	1951
11.37	590	10.98	929	13.19	1931
11.45	590	11.06	928	13.29	1946
11.55	589	11.14	948	13.39	1961
11.63	589	11.22	947	13.49	1942
11.71	588	11.31	946	13.58	1922
11.79	608	11.39	945	13.68	1920
11.87	608	11.47	924	13.78	1935
11.97	607	11.55	964	13.88	1915
12.06	585.79	11.64	942	13.98	1913
12.14	605.74	11.72	962	14.08	1946
12.22	605.18	11.80	981	14.18	1943
12.30	604.61	11.88	980	14.28	1941
12.40	583.49	11.98	959	14.38	1939
12.48	582.94	12.07	958	14.48	1937
12.57	582.39	12.13	937	14.57	1935
12.65	581.84	12.21	956	14.67	1932
12.73	581.30	12.30	935	14.77	1930
12.83	600.98	12.39	934	14.87	1928
12.91	600.42	12.46	954	14.97	1943
12.99	599.85	12.54	953	15.07	1941
13.08	619.57	12.64	972	15.17	1938
13.16	618.98	12.72	971	15.27	1953
13.26	638.52	12.81	970	15.37	1968
13.34	637.91	12.89	969	15.47	1949
13.42	637.31	12.97	968	15.56	1946
13.50	656.89	13.05	987	15.66	1927
13.59	656.26	13.14	966	15.76	1976
13.68	655.51	13.22	965	15.86	1974
13.77	675.01	13.30	984	15.96	1954
13.85	654.27	13.38	963	16.06	1969
13.93	653.64	13.47	963	16.16	1950
14.01	653.02	13.55	981	16.26	1964
14.11	672.31	13.63	980	16.36	1962
14.19	651.64	13.71	980	16.46	1943
14.28	671.02	13.80	959	16.55	1940

14.36	690.36	13.88	978	16.65	1938
14.44	689.70	13.96	1016	16.75	1953
14.52	689.04	14.04	996	16.85	1950
14.62	668.32	14.13	975	16.95	1931
14.70	667.67	14.21	974	17.05	1929
14.79	667.03	14.29	1012	17.15	1927
14.87	646.52	14.37	972	17.25	1924
14.95	665.74	14.46	991	17.35	1888
15.05	664.97	14.54	990	17.45	1903
15.13	664.33	14.62	950	17.54	1934
15.21	643.90	14.70	968	17.64	1915
15.30	663.04	14.78	967	17.74	1929
15.38	662.40	14.87	986	17.84	1927
15.48	681.35	14.95	985	17.94	1925
15.56	680.69	15.03	965	18.04	1956
15.64	680.02	15.11	983	18.14	1920
15.72	679.36	15.20	963	18.24	1934
15.81	678.70	15.28	962	18.36	1932
15.90	677.90	15.36	961	18.46	1946
15.99	677.24	15.44	979	18.55	1910
16.07	676.58	15.53	978	18.63	1941
16.15	695.48	15.61	997	18.73	1956
16.23	694.80	15.69	996	18.85	1969
16.33	674.45	15.77	975	18.93	1934
16.41	673.79	15.86	994	19.05	1948
		15.94	993	19.13	1930
		16.02	973	19.25	1960
		16.10	991	19.35	1957
		16.19	1009	19.43	1955
		16.27	1008	19.54	1952
		16.35	1007	19.64	1934
		16.43	987	19.74	1964
		16.48	967		

Rf	0.92
c	0.00
Pa	2116 psf
K	750
n	0.45

1/(σ1-σ3)ult

1.66E-03
1.00E-03
4.84E-04

Ei	B	σ3	Ei	B	σ3	Ei	B	σ3
514298.93	0.00	173.00	740580.37	0.00	389.00	1068236.49	0.00	878.00

Axial Strain	Deviator Stress	Hyperbolic σ1-σ3	Axial Strain	Deviator Stress	Hyperbolic σ1-σ3	Axial Strain	Deviator Stress	Hyperbolic σ1-σ3
0.00	129.36	0.0	0.00	57.82	0	0.00	36.32	0
0.08	362.42	248.2	0.08	172.30	378.6	0.10	663.62	699.4
0.18	408.65	365.1	0.16	469.67	548.8	0.20	1006.65	1044.8
0.26	454.87	416.1	0.25	537.89	645.6	0.30	1207.62	1250.7
0.35	477.75	449.0	0.33	628.84	708.0	0.40	1388.01	1387.4
0.43	500.59	471.9	0.41	696.80	751.6	0.50	1467.25	1484.8
0.51	523.39	488.8	0.49	741.85	783.8	0.59	1526.20	1557.7
0.61	522.87	504.1	0.58	786.82	808.5	0.69	1605.15	1614.3
0.69	545.62	513.9	0.66	808.94	828.1	0.79	1623.64	1659.5
0.77	568.32	521.9	0.74	808.27	844.0	0.89	1682.25	1696.5
0.86	544.71	528.6	0.82	830.33	857.2	0.99	1700.63	1727.3
0.94	567.38	534.2	0.91	852.36	868.3	1.09	1698.93	1753.3
1.04	566.81	539.9	0.99	851.65	877.7	1.19	1717.24	1775.6
1.12	589.42	544.0	1.07	850.94	885.9	1.29	1755.51	1794.9
1.20	588.93	547.5	1.15	872.89	893.0	1.39	1753.75	1811.8
1.28	588.44	550.7	1.24	872.16	899.3	1.49	1751.99	1826.7
1.37	587.95	553.4	1.32	894.05	904.8	1.58	1770.17	1840.0
1.45	587.46	555.9	1.40	893.31	909.8	1.68	1748.47	1851.8
1.55	586.87	558.6	1.48	892.56	914.2	1.78	1766.61	1862.5
1.63	586.38	560.6	1.57	891.81	918.3	1.88	1744.95	1872.1
1.71	585.89	562.4	1.65	891.07	921.9	1.98	1763.04	1880.9
1.79	608.31	564.1	1.73	890.32	925.2	2.08	1781.10	1888.8

1.88	584.91	565.6	1.81	912.08	928.3	2.18	1799.11	1896.2
1.97	607.19	567.2	1.90	888.83	931.1	2.28	1797.29	1902.9
2.06	606.68	568.5	1.98	888.08	933.7	2.38	1775.70	1909.1
2.14	583.34	569.7	2.06	887.33	936.1	2.48	1734.39	1914.9
2.22	582.85	570.8	2.14	886.59	938.3	2.57	1772.09	1920.3
2.30	582.36	571.8	2.23	885.84	940.3	2.67	1770.29	1925.2
2.40	**558.99**	572.9	2.31	885.09	942.2	2.77	1827.58	1929.9
2.48	558.52	573.8	2.39	884.35	944.0	2.87	1806.04	1934.2
2.57	535.31	574.6	2.47	883.60	945.7	2.97	1804.20	1938.3
2.65	534.86	575.4	2.55	882.86	947.3	3.07	1802.36	1942.1
2.73	534.41	576.2	2.64	904.43	948.8	3.17	1780.90	1945.7
2.83	533.87	577.0	2.72	903.66	950.2	3.27	1779.08	1949.1
2.91	510.76	577.6	2.80	902.90	951.5	3.37	1796.84	1952.3
2.99	510.33	578.2	2.88	879.87	952.8	3.47	1814.55	1955.4
3.08	532.51	578.8	2.97	945.85	953.9	3.56	1812.69	1958.2
3.16	532.06	579.4	3.05	900.60	955.1	3.66	1810.83	1961.0
3.26	531.52	580.0	3.13	877.63	956.1	3.76	1808.97	1963.6
3.34	553.62	580.5	3.21	899.07	957.1	3.86	1826.58	1966.0
3.42	530.62	581.0	3.30	920.47	958.1	3.96	1805.25	1968.4
3.50	552.68	581.4	3.38	897.54	959.0	4.06	1822.82	1970.6
3.59	552.21	581.9	3.46	941.03	959.9	4.16	1820.94	1972.7
3.68	574.12	582.3	3.54	896.01	960.7	4.26	1819.06	1974.8
3.77	573.63	582.7	3.64	895.09	961.7	4.36	1836.55	1976.7
3.85	573.14	583.1	3.71	916.55	962.3	4.46	1815.29	1978.6
3.93	572.65	583.5	3.79	893.71	963.0	4.55	1832.75	1980.4
4.01	572.16	583.8	3.87	937.02	963.7	4.65	1830.85	1982.1
4.11	571.57	584.2	3.97	892.03	964.5	4.75	1867.53	1983.7
4.19	571.08	584.5	4.05	891.26	965.2	4.85	1846.32	1985.3
4.28	570.59	584.8	4.14	890.49	965.8	4.95	1863.65	1986.8
4.36	592.42	585.1	4.20	933.80	966.3	5.05	1880.94	1988.3
4.44	614.21	585.4	4.30	910.90	967.0	5.15	1840.55	1989.7
4.54	613.58	585.7	4.37	910.27	967.4	5.25	1877.02	1991.1
4.62	590.79	586.0	4.45	887.59	967.9	5.35	1836.71	1992.4
4.70	612.52	586.3	4.55	908.55	968.6	5.45	1873.10	1993.66
4.79	589.77	586.5	4.63	907.76	969.1	5.54	1852.00	1994.88

4.87	567.06	586.7	4.71	906.98	969.5	5.64	1869.18	1996.06
4.97	566.48	587.0	4.78	884.52	969.9	5.74	1867.21	1997.20
5.05	543.83	587.2	4.88	905.41	970.4	5.84	1846.18	1998.30
5.13	565.49	587.4	4.96	926.41	970.9	5.94	1863.29	1999.37
5.21	565.00	587.6	5.03	904.00	971.2	6.04	1842.30	2000.40
5.30	564.51	587.8	5.13	924.81	971.7	6.14	1821.34	2001.40
5.39	563.93	588.1	5.21	902.27	972.1	6.24	1838.41	2002.37
5.48	563.44	588.3	5.29	923.20	972.5	6.34	1855.45	2003.31
5.56	562.95	588.4	5.37	900.70	972.9	6.44	1853.48	2004.23
5.64	562.46	588.6	5.46	921.59	973.2	6.53	1851.52	2005.11
5.72	561.97	588.8	5.54	942.44	973.6	6.63	1811.74	2005.97
5.81	539.49	589.0	5.62	898.35	973.9	6.73	1847.60	2006.81
5.90	538.93	589.2	5.70	940.80	974.2	6.83	1845.64	2007.62
5.99	538.46	589.3	5.79	918.38	974.5	6.93	1843.68	2008.41
6.07	537.99	589.5	5.87	874.42	974.9	7.03	1860.55	2009.18
6.15	515.61	589.6	5.95	938.33	975.2	7.13	1858.57	2009.92
6.23	515.16	589.8	6.03	894.43	975.5	7.23	1856.59	2010.65
6.33	514.62	589.9	6.12	915.17	975.7	7.33	1854.61	2011.36
6.41	536.01	590.1	6.20	892.86	976.0	7.43	1871.38	2012.05
6.50	535.54	590.2	6.28	913.56	976.3	7.52	1888.11	2012.72
6.58	535.07	590.3	6.36	912.76	976.6	7.62	1904.80	2013.37
6.66	534.60	590.5	6.44	954.84	976.8	7.72	1884.06	2014.01
6.76	534.03	590.6	6.53	954.00	977.1	7.82	1863.37	2014.63
6.84	555.30	590.7	6.61	953.16	977.3	7.92	1880.02	2015.24
6.94	532.99	590.9	6.69	952.32	977.6	8.02	1878.00	2015.84
7.01	554.32	591.0	6.77	951.48	977.8	8.12	1894.59	2016.41
7.09	575.51	591.1	6.86	929.29	978.0	8.22	1892.55	2016.98
7.19	553.24	591.2	6.94	949.80	978.2	8.32	1890.51	2017.53
7.27	509.47	591.3	7.02	948.96	978.5	8.42	1888.47	2018.07
7.35	509.02	591.4	7.10	948.12	978.7	8.51	1886.42	2018.60
7.43	530.17	591.5	7.19	947.27	978.9	8.61	1884.38	2019.11
7.52	551.28	591.6	7.27	946.43	979.1	8.71	1882.34	2019.62
7.62	550.69	591.7	7.35	924.35	979.3	8.81	1898.77	2020.11
7.70	550.20	591.8	7.43	944.75	979.5	8.91	1915.16	2020.59
7.78	571.23	591.9	7.52	943.91	979.7	9.01	1876.22	2021.06

7.86	570.72	592.0	7.60	943.07	979.9	9.11	1874.17	2021.52
7.94	570.21	592.1	7.68	942.23	980.0	9.23	1890.11	2022.06
8.04	548.14	592.2	7.76	941.39	980.2	9.31	1870.09	2022.42
8.13	569.09	592.3	7.85	940.55	980.4	9.41	1886.40	2022.85
8.21	547.16	592.4	7.93	939.70	980.6	9.52	1902.25	2023.36
8.29	546.67	592.5	8.01	938.86	980.7	9.62	1918.48	2023.77
8.37	524.80	592.5	8.09	938.02	980.9	9.70	1880.22	2024.10
8.47	545.59	592.6	8.18	958.23	981.1	9.80	1878.15	2024.50
8.55	545.10	592.7	8.26	936.34	981.2	9.92	1912.17	2024.97
8.63	544.61	592.8	8.34	935.50	981.4	10.02	1891.85	2025.35
8.72	544.12	592.9	8.42	934.66	981.5	10.12	1926.18	2025.72
8.80	543.63	592.9	8.51	933.82	981.7	10.22	1924.06	2026.09
8.90	521.78	593.0	8.59	932.98	981.8	10.32	1903.77	2026.45
8.98	521.31	593.1	8.67	932.13	982.0	10.42	1901.67	2026.81
9.06	520.84	593.2	8.75	931.29	982.1	10.51	1881.44	2027.15
9.14	520.37	593.2	8.83	930.45	982.3	10.61	1933.68	2027.49
9.23	519.90	593.3	8.92	908.73	982.4	10.71	1895.36	2027.83
9.33	519.33	593.4	9.00	949.63	982.5	10.81	1929.39	2028.16
9.41	518.86	593.4	9.08	948.77	982.7	10.91	1927.25	2028.48
9.49	518.39	593.5	9.16	927.09	982.8	11.01	1889.06	2028.80
9.57	517.92	593.6	9.25	947.05	982.9	11.11	1904.96	2029.11
9.65	517.45	593.6	9.33	925.41	983.0	11.21	1902.84	2029.42
9.75	516.89	593.7	9.41	924.56	983.2	11.31	1882.75	2029.72
9.84	537.46	593.8	9.49	944.47	983.3	11.41	1898.60	2030.02
9.92	536.97	593.8	9.58	943.61	983.4	11.50	1914.40	2030.31
10.00	536.48	593.9	9.66	963.46	983.5	11.60	1912.26	2030.59
10.08	556.97	593.9	9.74	962.58	983.6	11.70	1928.00	2030.87
10.16	556.46	594.0	9.82	941.03	983.7	11.80	1907.97	2031.15
10.26	555.85	594.0	9.91	940.17	983.9	11.90	1905.83	2031.42
10.35	555.34	594.1	9.99	959.94	984.0	12.00	1921.52	2031.69
10.43	554.83	594.2	10.07	959.07	984.1	12.10	1919.35	2031.96
10.51	575.20	594.2	10.15	958.19	984.2	12.20	1899.41	2032.21
10.59	553.81	594.3	10.24	977.89	984.3	12.30	1915.03	2032.47
10.69	574.04	594.3	10.32	976.99	984.4	12.40	1912.87	2032.72
10.77	573.51	594.4	10.40	935.01	984.5	12.50	1928.43	2032.97

10.86	572.98	594.4	10.48	954.67	984.6	12.59	1890.84	2033.21
10.94	572.45	594.5	10.57	974.29	984.7	12.69	1924.07	2033.45
11.02	571.93	594.5	10.65	952.91	984.8	12.79	1939.55	2033.69
11.12	571.29	594.6	10.73	931.57	984.9	12.89	1919.70	2033.92
11.20	591.49	594.6	10.81	971.60	985.0	12.99	1935.15	2034.15
11.28	570.23	594.7	10.90	950.28	985.1	13.09	1950.55	2034.37
11.37	590.39	594.7	10.98	928.99	985.1	13.19	1930.74	2034.60
11.45	589.84	594.7	11.06	928.13	985.2	13.29	1946.11	2034.82
11.55	589.18	594.8	11.14	947.64	985.3	13.39	1961.43	2035.03
11.63	588.64	594.8	11.22	946.76	985.4	13.49	1941.66	2035.24
11.71	588.09	594.9	11.31	945.88	985.5	13.58	1921.94	2035.45
11.79	608.13	594.9	11.39	945.00	985.6	13.68	1919.73	2035.66
11.87	607.56	595.0	11.47	923.83	985.7	13.78	1935.00	2035.86
11.97	606.88	595.0	11.55	963.52	985.7	13.88	1915.33	2036.06
12.06	585.79	595.0	11.64	942.37	985.8	13.98	1913.13	2036.26
12.14	605.74	595.1	11.72	961.72	985.9	14.08	1945.73	2036.46
12.22	605.18	595.1	11.80	981.05	986.0	14.18	1943.49	2036.65
12.30	604.61	595.2	11.88	980.13	986.1	14.28	1941.25	2036.84
12.40	583.49	595.2	11.98	958.85	986.1	14.38	1939.01	2037.03
12.48	582.94	595.2	12.07	957.95	986.2	14.48	1936.77	2037.21
12.57	582.39	595.3	12.13	937.09	986.3	14.57	1934.52	2037.40
12.65	581.84	595.3	12.21	956.34	986.4	14.67	1932.28	2037.58
12.73	581.30	595.3	12.30	935.34	986.4	14.77	1930.04	2037.75
12.83	600.98	595.4	12.39	934.28	986.5	14.87	1927.80	2037.93
12.91	600.42	595.4	12.46	953.64	986.6	14.97	1942.78	2038.10
12.99	599.85	595.5	12.54	952.75	986.6	15.07	1940.52	2038.27
13.08	619.57	595.5	12.64	971.70	986.7	15.17	1938.26	2038.44
13.16	618.98	595.5	12.72	970.78	986.8	15.27	1953.16	2038.61
13.26	638.52	595.6	12.81	969.86	986.9	15.37	1968.02	2038.77
13.34	637.91	595.6	12.89	968.95	986.9	15.47	1948.59	2038.93
13.42	637.31	595.6	12.97	968.03	987.0	15.56	1946.31	2039.09
13.50	656.89	595.7	13.05	987.04	987.0	15.66	1926.94	2039.25
13.59	656.26	595.7	13.14	966.20	987.1	15.76	1975.87	2039.41
13.68	655.51	595.7	13.22	965.28	987.2	15.86	1973.55	2039.56
13.77	675.01	595.8	13.30	984.24	987.2	15.96	1954.21	2039.71

13.85	654.27	595.8	13.38	963.45	987.3	16.06	1968.91	2039.86
13.93	653.64	595.8	13.47	962.53	987.4	16.16	1949.60	2040.01
14.01	653.02	595.8	13.55	981.43	987.4	16.26	1964.26	2040.16
14.11	672.31	595.9	13.63	980.49	987.5	16.36	1961.94	2040.30
14.19	651.64	595.9	13.71	979.56	987.5	16.46	1942.69	2040.45
14.28	671.02	595.9	13.80	958.86	987.6	16.55	1940.39	2040.59
14.36	690.36	596.0	13.88	977.69	987.6	16.65	1938.09	2040.73
14.44	689.70	596.0	13.96	1016.20	987.7	16.75	1952.65	2040.87
14.52	689.04	596.0	14.04	995.52	987.8	16.85	1950.33	2041.00
14.62	668.32	596.0	14.13	974.88	987.8	16.95	1931.18	2041.14
14.70	667.67	596.1	14.21	973.94	987.9	17.05	1928.88	2041.27
14.79	667.03	596.1	14.29	1012.31	987.9	17.15	1926.58	2041.41
14.87	646.52	596.1	14.37	972.07	988.0	17.25	1924.28	2041.54
14.95	665.74	596.2	14.46	990.75	988.0	17.35	1888.49	2041.67
15.05	664.97	596.2	14.54	989.79	988.1	17.45	1902.95	2041.79
15.13	664.33	596.2	14.62	949.69	988.1	17.54	1934.07	2041.92
15.21	643.90	596.2	14.70	968.33	988.2	17.64	1915.07	2042.04
15.30	663.04	596.3	14.78	967.40	988.2	17.74	1929.43	2042.17
15.38	662.40	596.3	14.87	985.98	988.3	17.84	1927.10	2042.29
15.48	681.35	596.3	14.95	985.02	988.3	17.94	1924.78	2042.41
15.56	680.69	596.3	15.03	964.59	988.4	18.04	1955.66	2042.53
15.64	680.02	596.4	15.11	983.11	988.4	18.14	1920.14	2042.65
15.72	679.36	596.4	15.20	962.72	988.5	18.24	1934.38	2042.76
15.81	678.70	596.4	15.28	961.78	988.5	18.36	1931.57	2042.90
15.90	677.90	596.4	15.36	960.85	988.6	18.46	1945.74	2043.02
15.99	677.24	596.5	15.44	979.29	988.6	18.55	1910.38	2043.13
16.07	676.58	596.5	15.53	978.34	988.7	18.63	1941.49	2043.22
16.15	695.48	596.5	15.61	996.73	988.7	18.73	1955.59	2043.33
16.23	694.80	596.5	15.69	995.76	988.7	18.85	1969.17	2043.46
16.33	674.45	596.5	15.77	975.48	988.8	18.93	1934.40	2043.55
16.41	673.79	596.6	15.86	993.81	988.8	19.05	1947.97	2043.68
			15.94	992.84	988.9	19.13	1929.68	2043.76
			16.02	972.61	988.9	19.25	1959.56	2043.89
			16.10	990.89	989.0	19.35	1957.16	2043.99
			16.19	1009.13	989.0	19.43	1955.23	2044.08

16.27	1008.14	989.0	19.54	1952.35	2044.20
16.35	1007.15	989.1	19.64	1933.67	2044.30
16.43	987.00	989.1	19.74	1963.80	2044.40
16.48	967.27	989.1			

Comparison Hyperbolic vs. Test Data (Deviator Stress vs. Axial Strain) - Soft Soil